

Development of a Microfluidic Hemodialysis Device Equipped with an Antifouling Nanoporous Dialysis Membrane

by

Kyle Alexander Chu

A thesis

presented to the University of Waterloo

in fulfilment of the

thesis requirement for the degree of

Master of Science

in

Chemistry

Waterloo, Ontario, Canada, 2021

© Kyle Alexander Chu 2021

Author's Declaration

I hereby declare that I am the sole author of this thesis. This is a true copy of the thesis, including any required final revisions, as accepted by my examiners.

I understand that my thesis may be made electronically available to the public.

Abstract

The loss of kidney function, or chronic kidney disease, causes over a million deaths worldwide every year. The ideal treatment would be a kidney transplant, however there are insufficient kidney donors for every patient that requires treatment. Therefore, the most common form of treatment is hemodialysis. Conventional hemodialysis is a large time commitment and is associated with various adverse effects. A wearable and continuous hemodialysis system can address many of these problems. This thesis aims to design a hemodialyzer that can be used such a system.

Using previous work as inspiration, various plate-type microfluidic designs were created to suit these needs. The geometry and dimensions were optimized by analyzing its microfluidics, as well as the restrictions in terms of fabrication and operation. A stackable serpentine design was determined based on these considerations. A track-etched polycarbonate membrane was chosen to be used in the hemodialyzer for its straightforward structure and superior performance compared to the cellulose membrane. This membrane is then functionalized with polyethylene glycol to provide antibiofouling properties which can help in decreasing the adverse effects experienced by the patient.

This thesis demonstrates that the performance of this polycarbonate membrane has a mass transfer coefficient of around $4.1 \mu\text{m/s}$, and when used in a continuous setting (168 hours/week) can be comparable to some commercial hollow-fibre hemodialyzers, such as the Fresenius F4 with a mass transfer coefficient of around $8.9 \mu\text{m/s}$ (12 hours/week). This research

provides a platform for the development of a continuous, wearable hemodialysis system that can provide adequate dialysis with the implementation of flow rates increased to that of a commercial system, and the employment of its modular design for an increased surface area.

Acknowledgements

I would like to thank Dr. Shirley Tang for her guidance throughout this project as well as the opportunity to pursue my graduate studies in her laboratory.

I would also like to thank my committee members, Dr. Juewen Liu and Dr. Vivek Maheshwari for their time and for providing feedback and guidance on my work.

Finally, I would like to thank all the past and current members of the Tang research group for all of their help and guidance.

Table of Contents

Author's Declaration	ii
Abstract	iii
Acknowledgements	v
List of Figures	viii
List of Abbreviations	ix
Chapter 1 — Introduction	1
1.1 The Kidney	1
1.2 Chronic Kidney Disease	2
1.3 Hemodialysis	4
1.4 Commercial Hemodialyzers	7
1.5 The Microfluidics of Hemodialysis	9
1.5 Objective of Project	12
1.6 Previous Work	13
Chapter 2 — Design and Fabrication of the Microfluidic Hemodialyzer	14
2.1 Optimization of Hemodialyzer Configuration	14
2.2 Optimization of Channel Dimensions	18
2.2.1 Fabrication Methods	21
2.3 Hemolysis Simulations	23
Chapter 3 — Prototype Hemodialyzer and Performance Evaluation	26
3.1 Introduction	26
3.2 Materials and Methods	27
3.2.1 Cellulosic Membranes	27
3.2.2 Polycarbonate Membranes	29
3.2.3 Experimental Methods	30
3.2.4 Assays	33
3.3 Experimental Results and Discussion	34

3.3.1 Urea and Albumin Clearance	34
3.3.2 Discussion of Hemodialyzer Performance	43
Chapter 4: Membrane Surface Functionalization.....	47
4.1 Introduction.....	47
4.2 Materials and Methods	49
4.3 Experimental Results and Discussion	50
Chapter 5: Summary and Future Work.....	52
5.1 Summary	52
5.2 Future Work	53
5.2.1 Pore Size Manipulation	53
5.2.2 Dialysate Regeneration.....	53
5.2.3 Blood–plasma separation	54
5.2.4 Other Solutes	55
References	56
Appendices.....	62
Appendix A: Reduction of Membrane Thickness	62
Appendix B: Creatinine Assay.....	65

List of Figures

Figure 1. Schematic of the flow in a kidney and nephron.	2
Figure 2. Schematic diagram of water treatment and hemodialysis.	4
Figure 3. Cocurrent flow compared to countercurrent flow.	5
Figure 4. Various microfluidic channel designs.	16
Figure 5. The wide channel serpentine channel design.	21
Figure 6. Schematics of dialysate and blood flow.	23
Figure 7. Shear stress simulation of the entire microfluidic channel.	24
Figure 8. SEM images of the cellulose membrane.	29
Figure 9. SEM images of the polycarbonate membrane.	30
Figure 10. The dialysate urea concentration of the cellulose membrane hemodialyzer.	35
Figure 11. The urea clearance of the polycarbonate membrane hemodialyzer.	37
Figure 12. The urea clearance of the polycarbonate membrane hemodialyzer with reduced dialysate volume.	38
Figure 13. The urea clearance of the polycarbonate membrane hemodialyzer with BSA.	39
Figure 14. The BSA clearance of the polycarbonate membrane hemodialyzer.	39
Figure 15. The urea clearance of the polycarbonate membrane hemodialyzer in whole blood.	43
Figure 16. General scheme of the reaction between APTES and cellulose.	48
Figure 17. Scheme of membrane functionalization using EDC–NHS carbodiimide chemistry. ...	49
Figure 18. Scheme of the amination of polycarbonate.	50
Figure 19. Contact angles of the polycarbonate membrane.	51

List of Abbreviations

3D	three-dimensional
ABS	acrylonitrile butadiene styrene
APTES	(3-aminopropyl)triethoxysilane
BMF	blood-mimicking fluid
BSA	bovine serum albumin
CKD	chronic kidney disease
EDC	1-ethyl-3-(3-dimethylamino-propyl)carbodiimide
ESRD	end-stage renal disease
GFR	glomerular filtration rate
HMDA	hexamethylenediamine
KoA	mass transfer–area coefficient
NHS	N-hydroxysuccinimide
PBS	phosphate-buffered saline
PDMS	polydimethylsiloxane
PEG	polyethylene glycol
PMMA	poly(methyl methacrylate)
RRT	renal replacement therapy
SEM	scanning electron microscope
UV–vis	ultraviolet–visible
WAK	Wearable Artificial Kidney™

Variables:

A	surface area
C	concentration
D	diffusion coefficient
d_m	pore diameter

G	generation rate
h	height
J	flux
K	solute clearance
K_0	mass transfer coefficient
K_p	partition coefficient
L	length
P	pressure
Q	flow rate
R_h	hydraulic resistance
t	time
V	volume
w	width
$\dot{\gamma}$	shear rate
ε	porosity
μ	dynamic viscosity
τ	tortuosity

Subscripts:

B	blood <i>or</i> blood-mimicking fluid
D	dialysate
pre	pre-dialysis
$post$	post-dialysis
uf	ultrafiltration
w	wall
0	initial

Chapter 1 — Introduction

1.1 The Kidney

The kidneys are important organs that serve to eliminate waste, regulate electrolyte levels, and blood volume.¹ The functional unit of the kidney is the nephron which performs these functions.² The blood enters the glomerulus where it is filtered through into the Bowman's capsule.² This filtrate then travels through various ducts and loops to undergo selective solute reabsorption and secretion of waste products into and from the circulation.² This final filtrate is then transported to the bladder for excretion.² These selective reabsorption and secretion steps allow the elimination of waste as well as the regulation of physiological parameters. This eliminated waste includes both endogenous waste products as well as exogenous drugs and toxins.¹ Of these endogenous waste products eliminated by the kidneys, urea is the most abundant and originates as a product of protein metabolism.^{3, 4} After proteins are metabolized into their substituent amino acids, they are deaminated to form ammonia.⁴ To prevent the toxic effects of the ammonia, it is converted in the liver into the less harmful compound urea, which is then excreted via the kidneys.⁵ Human kidney function is estimated by the glomerular filtration rate (GFR), with normal values around 120–130 mL/min/1.73 m² in younger populations, declining with age.⁶ However, with reduced GFR, urea and other waste products accumulate in the blood, resulting in uremia, which is mainly associated with chronic kidney disease (CKD).⁷

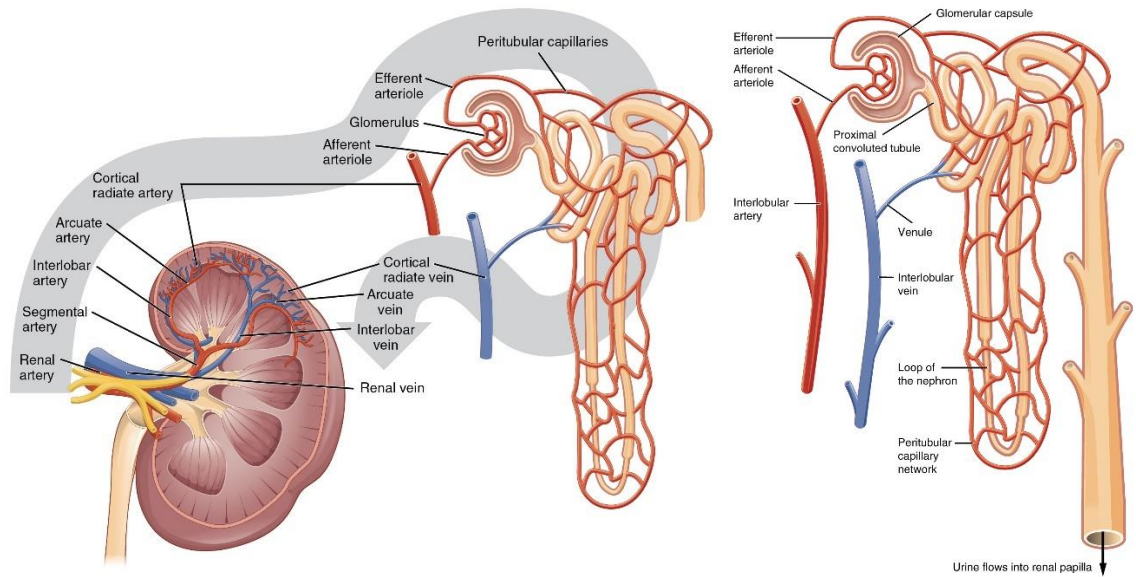


Figure 1. Schematic of the flow in a kidney and nephron. The left shows the general flow within the kidney, with the right showing the flow within the nephron.⁸

1.2 Chronic Kidney Disease

Chronic kidney disease is a condition where a patient has an irreversible loss of kidney function that occurs over months or years.⁹ Its formal definition as defined by international guidelines is the exhibition of markers of kidney damage such as albuminuria or structural abnormalities, or a GFR of less than 60 mL/min/1.73 m², or both, sustaining over at least three months.⁹ Chronic kidney disease is prevalent, with an estimated 697 million people suffering from it worldwide in 2019, where the regions of North America, Latin America-Caribbean, Europe-Central Asia, and East Asia-Pacific have a prevalence rate of over 10% of the population.¹⁰ In the same year, there were an estimated 1.43 million deaths from CKD worldwide, constituting over 2.5% of global deaths.¹⁰ Chronic kidney disease is categorized into stages based on kidney function. The fifth and final stage of CKD, also known as end-stage renal disease (ESRD), is defined

as a GFR below 15 mL/min/1.73 m² and the kidney is considered to be no longer able to sustain the patient's life in the long term.⁹ When a patient has ESRD, they need to be treated with a form of renal replacement therapy (RRT), which includes hemodialysis and renal transplantation.¹¹

There were an estimated 2.6 million patients receiving RRT worldwide in 2010, approximately 2.1 million of which were receiving dialysis.¹¹ While renal transplantation is generally more ideal, there is a severe shortage of kidney donors with only around 16% of American ESRD patients receiving a transplantation in 2017, resulting in the large majority of patients undergoing hemodialysis.^{12, 13} It was also estimated that there were between 4.9–9.7 million patients who required RRT in 2010, while only around 2.6 million people were receiving it.¹¹ This suggests that there are millions of patients who are not receiving the treatment that they need.¹¹ The use of RRT worldwide was projected to more than double to around 5.4 million people by 2030, but the patients that will still be unable to access RRT will remain a significant proportion of the population as the number of people requiring it will increase as well.¹¹ The largest disparity between the number of patients needing and receiving RRT in terms of geographical region is Africa, followed by Asia, and in terms of income levels, low-income families, followed closely by the lower-middle income level.¹¹ Even at the upper-middle income level, the number of patients requiring RRT was around two to five times the number of patients receiving it.¹¹ This makes it abundantly evident that there is an urgent need for the development of RRT that has a lower cost and is more accessible to everyone.

1.3 Hemodialysis

Hemodialysis is a procedure in which blood from a patient is passed through a hemodialyzer to remove uremic waste and excess fluids.¹⁴ This hemodialyzer contains a semipermeable membrane between the blood and the dialysate – a buffer and electrolyte solution with similar concentrations as in blood that is used to collect the waste.¹⁵ The solutes diffuse from the blood to the dialysate along a concentration gradient.¹⁵ Typically, to maximize the concentration gradient between the blood and the dialysate, they are made to flow in opposite directions, or countercurrently.¹⁶ With countercurrent flow, the maximum possible clearance would be 100%, whereas with cocurrent flow, the maximum possible clearance would only be 50% since it will reach equilibrium (Figure 3).

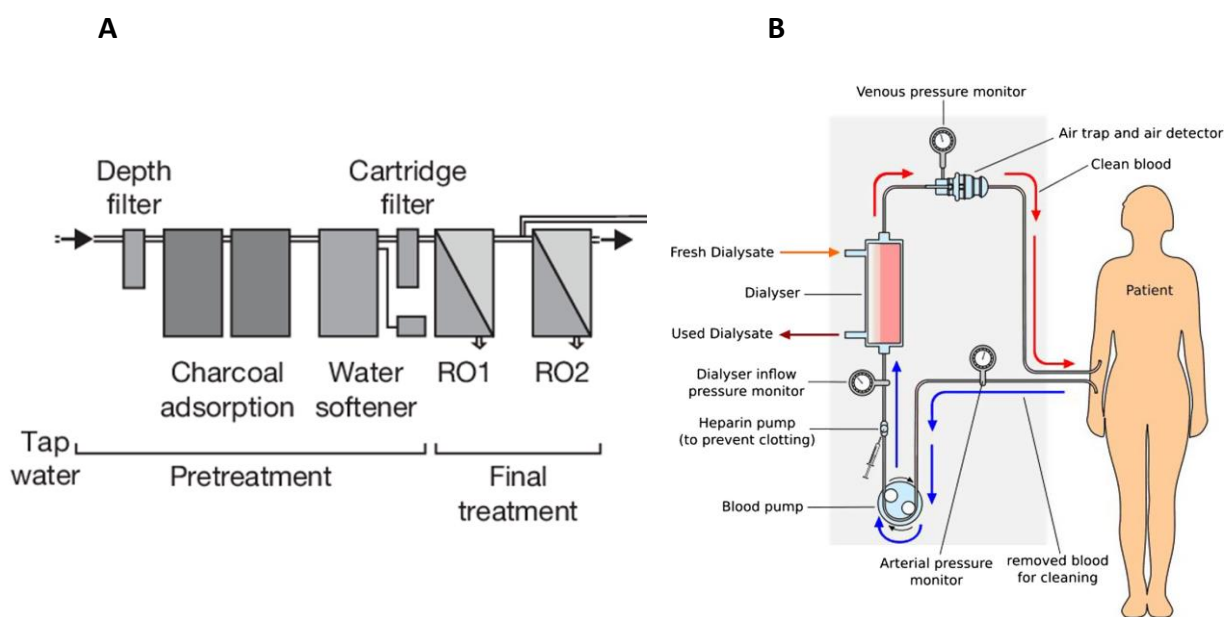


Figure 2. Schematic diagram of water treatment and hemodialysis. The left (A) depicts an example of the treatment required to purify water for the making dialysate prior to adding electrolytes and storage in large tanks.¹⁷ RO1 and RO2 are two reverse osmosis systems.

Copyright © 2007 Karger Publishers, Basel, Switzerland. The right (B) depicts a general schematic of hemodialysis.¹⁸

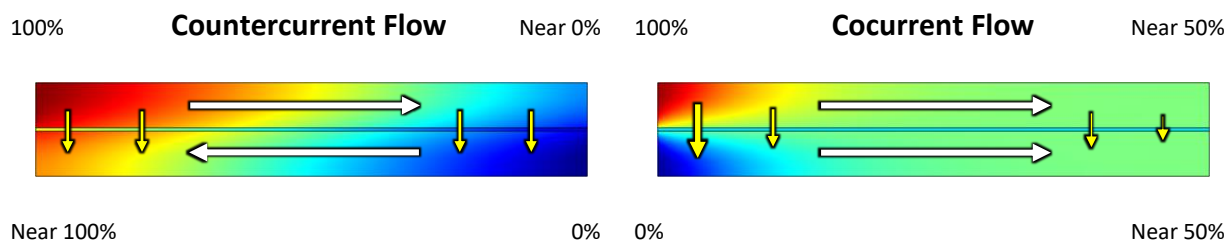


Figure 3. Cocurrent flow compared to countercurrent flow. The percentage refers to the concentration of diffusible solutes in solution, with 100% (red) being the concentration in the blood prior to dialysis, and 0% (blue) being the concentration in the dialysate prior to dialysis.

Hemodialysis was used to treat almost 90% of all new patients of ESRD in the United States in 2020 and has been significantly increasing the probability of survival of these patients.¹⁹ However, conventional hemodialysis devices are considerably large and cumbersome devices that require physicians and nurses to operate, an extensive water purification system (Figure 2A), and treatment quality management, so these are usually situated in a hospital or dialysis centre, where patients will go to for dialysis treatments lasting for around 3–4 hours per session, three times a week.^{20, 21} This considerable time commitment can significantly reduce the patient's quality of life, which, as a result, increases the rate of noncompliance and nonadherence to the treatment schedule.²² Additionally, the frequency of conventional hemodialysis has been demonstrated to be insufficient since urea and other toxins can accumulate significantly between hemodialysis treatment sessions. The accumulation of these toxins is significant enough to cause uremic symptoms in hemodialysis patients.²³

In contrast, portable hemodialysis devices are able to mitigate many of these issues. Since the device is connected to the patient, there should be no problems with the time commitment required for hemodialysis treatment, and of course, the associated nonadherence. Portable hemodialysis can give patients freedom of movement and allow them to engage in everyday activities that would otherwise be impossible for them. More frequent hemodialysis sessions have been shown to alleviate the uremia associated with conventional hemodialysis,²³ and therefore, a portable device that dialyzes the blood continuously should prevent any uremic symptoms. In addition to uremia, daily hemodialysis has also been shown to better control blood pressure and hematocrit problems to the point where some patients were able to reduce or discontinue taking antihypertensive drugs and erythropoietin, respectively.²⁴ Daily hemodialysis was also shown to have beneficial effects on nutrition, mental health, energy, patient survival, and decreased morbidity.²⁵ Likewise, it was shown to improve the patient's long-term health-related quality of life, such as physical and social functioning and vitality.²⁶ Frequent hemodialysis can also prevent the occurrence of dialysis disequilibrium syndrome. This syndrome, while uncommon, is a very serious complication of hemodialysis – patients during or immediately after their hemodialysis treatment may experience neurological deterioration, with symptoms suggestive of increased intracranial pressure including restlessness, mental confusion, and coma.²⁷ While this syndrome is not well understood, it is thought that if a significant amount of urea is removed during hemodialysis, an osmotic pressure gradient can be generated between the brain, an area where urea diffuses more slowly, and the blood.²⁷ Continuous hemodialysis in

the form of a portable hemodialysis system can prevent these large interdialytic fluctuations of uremic toxins, which in turn can reduce these problems.

Portable hemodialysis devices are already being developed by other groups, the most well-known of which is the Wearable Artificial Kidney™ (WAK). The WAK is a complete hemodialysis system that is situated on a belt and includes pumps for blood and dialysate flow, as well as pumps for fluid removal and infusion of substances such as heparin.^{28, 29} It uses a commercially available hemodialyzer and has a system to regenerate the dialysate, therefore only requiring 400 mL of dialysate.²⁸ Similar systems such as those developed by Nanodialysis and EasyDial are also based on a commercially available dialyzer.^{30, 31}

1.4 Commercial Hemodialyzers

Commercially available hemodialyzers typically use synthetic materials such as polysulfones or polyethersulfones, and usually make use of hollow fibre membrane systems, where the blood flows through the hollow centre of the fibre and the dialysate flows countercurrently in a large chamber which encloses all of the hollow fibres.³² However, these membranes can have many drawbacks.

Polysulfone and polyethersulfone membranes are hydrophobic, which can cause membrane biofouling by allowing the adsorption of proteins and other nonpolar or hydrophobic particles, as well as bacteria onto the surface of the membrane.^{33, 34} Biofouling is not ideal for two main reasons. Firstly, when there are proteins or other foulants covering the exchange surface, the ability of the hemodialyzer to remove the solutes decreases.³⁵ Secondly, when

proteins and blood cells are adsorbed onto the hemodialyzer surface, immune responses can be triggered.³⁵ This tendency of experiencing membrane fouling is compounded with the usage of a hollow fibre membrane system. This membrane configuration intrinsically has a higher frequency of membrane fouling, in part due to the internal diameter of each fibre being only 200 μm and each dialyzer having large surface areas of 1–2 m^2 .^{32, 36, 37}

The manufacturing processes used to fabricate the hollow fibre membranes are also more expensive relative to other types of membrane systems.³⁶ This results in an increased cost for the entire hemodialyzer which in turn lends to higher reuse of the same hemodialyzer in a clinical setting. While hollow fibre hemodialyzers are designed to be reused, there exists the concern that the disinfection required between uses may leave residual chemicals which are harmful to the patient.³⁸ Furthermore, the chemicals that are used in the disinfection process may alter the membrane integrity and allow blood proteins such as albumin to cross the membrane.³⁹ These concerns are realized in a meta-analysis on hemodialyzer reuse which shows an increased relative risk of hospitalization when the dialyzer was reused.⁴⁰ There is also the potential problem of inconsistent flow control since there are approximately 10,000 hollow fibre which cannot be controlled individually.³⁷ Zones of lower flow rates can decrease clearance or even result in increased fouling due to the increased residence time in the hemodialyzer.⁴¹ Conversely, there may be certain fibres with much higher speeds, exerting a larger shear stress, which could result in shear-induced hemolysis.⁴²

Synthetic membranes are typically considered to be biocompatible in hemodialysis as compared to other types of membranes.⁴³ One common method of testing the biocompatibility

is investigating its complement activation. The complement system is a part of the immune system which initiates phagocytosis to remove bacteria and attacks their cell membranes.⁴⁴ There are multiple paths that can trigger the complement system, but they all eventually result in the cleavage of complement component 3, C3.⁴⁵ When this occurs, a cascade of enzymatic cleavages occur which ultimately leads to the formation of pores in the pathogen membrane and its cell death.⁴⁵ However, the activation of this complement system leads to inflammation and can also damage host tissues, so ideally, it is not triggered during hemodialysis.⁴⁵

1.5 The Microfluidics of Hemodialysis

In order to optimize the performance of the hemodialyzer, it was necessary to investigate the mechanisms behind the process of hemodialysis. The transport of the solutes (such as urea) from the blood to the dialysate primarily occur via a combination of two mechanisms: diffusion and convection.⁴⁶

In diffusion-based transport, the solute is transported across the membrane mainly by its chemical concentration gradient.⁴⁶ This solute flux can be described by Equation 1:

$$J_{diffusion} = \frac{K_p \cdot D \cdot \varepsilon \cdot \Delta C}{L} \quad (1)$$

where K_p is the membrane solute partition coefficient, D is the membrane solute diffusion coefficient, ε is the membrane porosity, ΔC is the transmembrane concentration gradient, and L is the membrane thickness.⁴⁷ The solute travels down its concentration gradient (from the side of higher concentration to the side of lower concentration) due to random molecular movement.⁴⁸ Diffusive clearance is independent of fluid flow, and occurs naturally without any

flow through the membrane, in which case, the concentration on either side would eventually equilibrate and become the same. In hemodialysis, most of the uremic waste is removed via diffusion.⁴⁸

In convection-based transport, the solute is transported along with its solvent and is driven mainly by the transmembrane pressure gradient in the process of ultrafiltration.⁴⁶ In the case of hemodialysis, the solvent would be the blood plasma (without any of the components that are unable to pass the membrane, such as large proteins). This permeate flux can be described by Equation 2:

$$J_{convection} = \frac{\Delta P}{\mu R_h} \quad (2)$$

where ΔP is the transmembrane pressure, μ is the dynamic viscosity of the fluid, and R_h is the membrane hydraulic resistance.⁴⁹ Convective clearance is independent of any solute concentrations and can even occur without any solute since it is simply the transport of fluid according to the transmembrane pressure gradient. This transmembrane pressure is the observed difference in pressure between the blood and dialysate sides, and it consists of two components. The first component is the difference in pressures of the blood and dialysate channels.⁴⁶ The second is the osmotic pressure gradient generated by the blood proteins and other molecules found in the blood.⁴⁶ This pressure acts in the direction opposite to the desired direction of filtration due to the much lower concentration of solutes in the dialysate, but fortunately, does not overcome the dynamic pressure. Additionally, in order to cause more convection, the transmembrane pressure can be manipulated. One way of accomplishing this is

to increase the blood flow rate to increase the dynamic pressure on the blood side, which would increase the transmembrane pressure.⁴⁶ Similarly, the pressure on the dialysate side can be reduced to increase the transmembrane pressure to increase the convective clearance. In commercial hemodialysis systems, the pressure on the dialysate side is decreased to increase the convective clearance in a process called ultrafiltration.

Countercurrent flow is nearly universally used in hemodialysis. Therefore, the pressure difference across the membrane changes along the length of the channel. At the end where the blood enters at high pressure and the dialysate leaves at low pressure, the pressure gradient drives the solutes towards the dialysate side. However, at the end of the dialyzer where the dialysate enters at high pressure and the blood leaves at low pressure, the pressure gradient is reversed, and the solutes are driven towards the blood side, causing so-called back-filtration.⁵⁰ Back-filtration is not an issue in terms of clearance, as the dialysate on the side that experiences back-filtration should essentially have no uremic toxins yet. However, it can be an issue since any impurities within the dialysate such as endotoxin fragments and bacterial substances can enter the blood stream of the patient, which can happen even when the bacterial counts and endotoxin concentrations are well within accepted concentrations.⁵¹

Another more comprehensive equation can be used to describe permeate flux and essentially expands upon the hydraulic resistance term in Equation 2:

$$J_{convection} = \frac{\varepsilon \cdot d_m^2}{32 \cdot L \cdot \tau} \frac{\Delta P}{\mu} \quad (3)$$

where ε is the porosity, d_m is the pore size, L is the membrane thickness, and τ is the tortuosity.⁵² This formula elaborates by showing how the convective clearance is dependent on the membrane pore size as well as the membrane thickness. The tortuosity term describes how convoluted the path may be for the molecules to diffuse from one side to another. This shows that the performance of the hemodialyzer is dependent on the membrane pore sizes, with a higher pore size leading to higher clearance. However, it is very important to carefully control the pore sizes of the membrane as they control not only which solutes can pass, but perhaps more importantly, which solutes remain in the blood. There are many important molecules in the blood which need to be retained, including proteins such as albumin. Therefore, pore sizes of the membrane must be large enough to allow uremic waste to pass, but small enough to retain these important molecules. Additionally, due to the dependence of both the diffusive and convective clearance on the membrane thickness, it would be ideal to minimize the thickness of the membrane to maximize the clearance.

1.5 Objective of Project

The objective of the overall project is to create a functional portable hemodialysis system using a microfluidic platform. More specifically, for this project, the primary objective was to design a well-functioning microfluidic hemodialyzer which would be usable in a wearable hemodialysis system and is able to remove urea and other uremic waste, with little loss of larger physiologically important molecules. With this design, a method of fabricating the hemodialyzer would need to be developed to create a consistent and durable dialyzer and a protocol for testing the dialyzer would also need to be created. The fabrication process and testing of the dialyzer

would need to be able to accommodate changes so that any future innovations will be able to be fabricated and tested in a similar fashion and be comparable to previous data.

1.6 Previous Work

Previous work has been done by members of this group on a microfluidic hemodialyzer.⁵³ Their design was modeled to mimic the function of the renal corpuscle. It was made from two polydimethylsiloxane (PDMS) chambers separated by a regenerated cellulose membrane. Similar to a renal corpuscle, one side was designed to have winding channels for the blood-mimicking fluid (BMF), to mimic the complex network of blood vessels in the glomerulus. The other side was designed to be one large chamber for the dialysate to mimic the Bowman's capsule. As with most other hemodialysis systems, the direction of the flow was countercurrent to generate a larger concentration gradient across the membrane for optimal clearance. The entire device was assembled and held together using a poly(methyl methacrylate) (PMMA) casing.

Chapter 2 — Design and Fabrication of the Microfluidic Hemodialyzer

2.1 Optimization of Hemodialyzer Configuration

Using the previous work as inspiration for its configuration, more designs were made and experimented with to optimize its geometry and other specifications to achieve a better hemodialysis performance. Many various designs were experimented with since the original rectangular channel design.

The first problem that was identified was the lack of flow control in the dialysate side of the hemodialyzer – the part mimicking the glomerulus. Due to its large chamber design, which was essentially an extremely wide channel, contrasted with the narrow tubing used for the inlets and outlets of this chamber, large portions of this chamber were dead zones. The flow in these regions was minimal and any solutes that had diffused into these areas were not efficiently removed from the system. This results in a decreased performance in the hemodialyzer. This is also a problem faced by conventional hemodialyzers where the inlets and outlets are commonly both on one side of the hemodialyzer.⁵⁴ This has been addressed in more recent hemodialyzers by employing a so-called moiré pattern, where each hollow fibre is made with a slightly undulating shape to decrease the amount of contact between adjacent fibres.⁵⁴ This pattern is able to diffuse the dialysate flow, yielding a more homogeneous dialysate flow distribution within the dialyzer.⁵⁴ Since this is not possible in hemodialyzers with a plate-like configuration, the flow had to be controlled by other means. Therefore, designs with the dialysis channels mirrored from the blood channels were made.

With the configuration of the blood and dialysate channels decided, the specific geometry of the channels needed to be improved. Many designs were considered for the channels, however only a few were experimentally tested. One such design was a branched serpentine structure (Figure 4A). This design was created to maximize the usage of the membrane surface area within one hemodialyzer unit. This design was tested for its urea clearance, which was around 0.070 mL/min with a flow rate of 10 mL/min in both the dialysate and BMF channels. The BMF side flow rate was adjusted to four times the original flow rate in an attempt to increase the transmembrane pressure and, in turn, the clearance, however the clearance seemed to decrease instead. This suggested that there may not have been any convective clearance and that the reduced residence time of the BMF in the dialyzer resulted in lower diffusive clearance. The ultrafiltration was then analyzed for confirmation by measuring the volumes before and after dialysis. However, the volumes did not measurably change over the course of over three hours, indicating that there was very little convective clearance, if any at all.

The beaded design (Figure 4B), which was originally designed with the intention of inducing vortices to increase the mixing within the channel and convective clearance, as well as the square design (Figure 4C), which resembled the design of the previous work, were then tested under the same conditions. The beaded design performed slightly better than the square design, but most likely only due to the increased amount of exposed membrane surface area. When taking the surface area into consideration, the beaded design had a much lower clearance compared to the square design. Additionally, the branched serpentine design performed better than the square design even when taking into consideration the increased surface area. These

results determined that any future designs should be more similar to the serpentine design than the other two since superfluous designs seemed to only yield more dead zones in the flow and inefficient use of the membrane surface area.

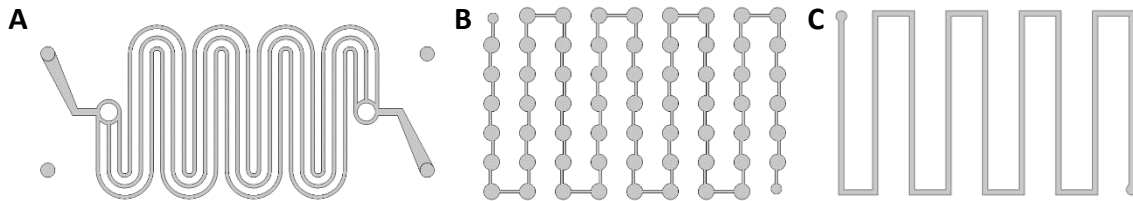


Figure 4. Various microfluidic channel designs. The opposite side is mirrored, with some slight changes to accommodate different flow paths. These designs are referred to as branched serpentine (A), beaded (B), and square (C).

Additionally, the option of increasing the surface area of the hemodialyzer without changing the geometry of the design was considered. This could be achieved by stacking multiple layers of the channels. With this implementation, further changes needed to be made to the overall configuration of the channels. Previously, the BMF had entered on the same face of the hemodialyzer as it exited, and likewise for the dialysate, but on the opposite face. However, to accommodate the option of stacking multiple layers, it would be ideal for the inlets of both the BMF and dialysate to enter from the same face, and the outlets to exit from the opposite face. This way, the outlets of the first unit can flow directly into the next unit. This was accomplished by designing the channels such that the BMF and dialysate channels would split apart at either end. Since they no longer occupied the same vertical space, they could be extended into the next layer. The stacked units can also be aligned to flow in series or in parallel. By aligning the outlets to their respective inlets, the length of the channel is effectively multiplied by the number of

stacked units. This would allow more waste to be removed from the blood before it leaves the hemodialyzer. On the other hand, by aligning the respective inlets and outlets with each other, the resulting hemodialyzer would closer resemble having multiple hemodialyses running concurrently. In a hemodialyzer that is stacked in series, each set of two layers would be flowing countercurrently with respect to each other, however the layers in between these two sets would be flowing cocurrently. This will result in reduced performance as the concentration gradient in cocurrently flowing channels is lower than that of countercurrently flowing channels. However, in a hemodialyzer stacked in parallel, all adjacent layers would be flowing countercurrently, resulting in the middle BMF channels having double the surface area due to having a dialysate channel on either side. This should result in an increased performance compared to stacking the layers in series. Furthermore, a hemodialyzer in parallel would be able to support a higher overall flow rate than one in series as there are more channels for the solution to flow through. So, for stacked-unit hemodialyzers, a parallel configuration is preferred over a series one. The addition of this feature also affects the geometry of the channels. Since the middle channels in the stack need to be through-cut, branching channels will be difficult to properly align as the design would then contain floating pieces. Therefore, the final channel geometry must be unbranched.

To conclude, the BMF and dialysate channels will be mirrored versions of each other for better flow control, with a diverging portion at either end so that the inlets and outlets can each be on one face of the hemodialyzer. The geometry of the channels will be serpentine to effectively use of the membrane surface area, but unbranched to allow for the option of stacking multiple layers.

2.2 Optimization of Channel Dimensions

After the overall geometry of the channels was determined, it was necessary to optimize the dimensions of these channels so that they would yield the most optimal hemodialysis efficiency. These optimizations were determined by analyzing various microfluidic equations as well as using computational simulations. These designs were further narrowed by considering the ease of fabrication as well as the price and availability of these materials. The dimensions of the channels were decided upon when the hemodialyzer was still fabricated with PDMS channels, with the option of additional inner layers made of through-cut PMMA for a stacked design, so both materials were taken into consideration.

The height of the channel was simply chosen to be as small as possible to maximize its aspect ratio and thereby maximize the surface area which could be in contact with the dialysis membrane for exchange. If the height of the channel is too large, the bulk solution flowing through the channel will not dialyze efficiently. For the 3D-print molded PDMS channels, the height was only limited by the layer height of the 3D printer, along with considerations of the deformation of the PDMS which could cause the channel to be smaller when compressed. However, for the PMMA channels, the height is mainly limited by the handleability of the PMMA sheets used in the fabrication. With PMMA sheets that are too thin, such as 0.3 mm PMMA, the pieces become too fragile to use consistently in fabrication. Since the PMMA would be the limiting factor for the height of the channel, it was determined that the channel height would be 0.5 mm for both the PDMS and PMMA channels for consistency, and that the relatively durable 0.5 mm PMMA would be used.

With the height of the channels established, the width of the channels was next to be determined. The width of the microfluidic channel was mainly constrained by the shear stress that would be experienced by the blood at the walls of the channels. Under high shear stress, the erythrocytes in the blood are susceptible to hemolysis. The threshold for hemolysis has been demonstrated to be around 1500 dyne/cm².⁴² Therefore, in order to minimize the amount of hemolysis in the hemodialyzer, the dimensions of the channel must be designed such that the maximum shear stress within does not exceed this threshold. For the incompressible two-dimensional flow of a Newtonian fluid in a rectangular channel where the width is significantly larger than the height, the wall shear rate can be modeled by the following equation:⁵⁵

$$\dot{\gamma}_w = \frac{6Q}{wh^2} \quad (4)$$

The wall shear stress, therefore, would be this value multiplied by the dynamic viscosity of the fluid. Since blood is a shear-thinning fluid, this value can serve as the upper limit of the wall shear stress experienced by the blood. Based on this equation, with a fixed height and flow rate, the wall shear stress decreases as the channel width increases. This is consistent with the intuition that the velocity will decrease with a larger cross-sectional area. With this analysis, multiple designs were made with increasing channel widths. The designs that used channel widths that were too large resulted multiple issues. The spacing between the turns of the channels needed to be relatively large in order to have sufficient structural integrity of the material for ease of handling and fabrication, which resulted in inefficient use of the membrane surface area. Furthermore, the wide channels required large diameter tubing for the inlets of the hemodialyzer to maintain a laminar flow as it enters the microfluidic channels. Large diameter tubing could

result in larger volumes of blood being required to fill the system, and in turn, more blood removed from the patient while in use. Based on these factors, a channel width of 3 mm was chosen, especially since it would be easily compatible with the common 1/8" inner diameter tubing.

Finally, the length of the channels needed to be defined. This was determined by the maximum pressure that the assembled device could handle before failure of the adhesive holding the device together. In order to determine this, the pressure drop of the microfluidic channel was estimated mathematically. The main failure point of the design at the time was between the molded PDMS and the membrane, which was secured using a double-sided adhesive. Therefore, the phenomenon that was investigated to signify the whether the adhesive bond had failed was the formation of Saffman–Taylor fingers. Saffman–Taylor fingers are dendritic structures that develop at the interface between a between two fluids when the less viscous fluid displaces the more viscous fluid. In this case, the fingers can form when the water displaces the adhesive at high pressures. The maximum pressure that an adhesive bond between PDMS and adhesive tape was determined by Thompson et al. to be around 200–350 kPa for three different brands of adhesive tapes.⁵⁶ The length was calculated using the lower end of this range, since we were unable to ascertain the pressures that our own adhesive could withstand. The viscosity of human whole blood has been demonstrated to be around 2.8 to 7.3 cP for shear rates from 1,000 to 1 s^{-1} .⁵⁷ Using fairly generous numbers for each parameter to ensure that the threshold for the formation of these fingers, the maximum length of the channel was determined using the Hagen–Poiseuille equation (Equation 5). This was further rounded down to 60 cm, since additional tubing

will need to be attached to the outlet of these channels, which would itself add to the pressure of the system.

$$L = \frac{h^3 w \Delta P}{12 \mu Q} \left(1 - 0.630 \frac{h}{w} \right) \quad (5)$$

$$L = \frac{(0.5 \text{ mm})^3 (3 \text{ mm}) (200 \text{ kPa})}{12 (8 \text{ mPa}\cdot\text{s}) (45 \text{ mL/min})} \left(1 - 0.630 \left(\frac{0.5 \text{ mm}}{3 \text{ mm}} \right) \right) \approx 93 \text{ cm} \quad (6)$$

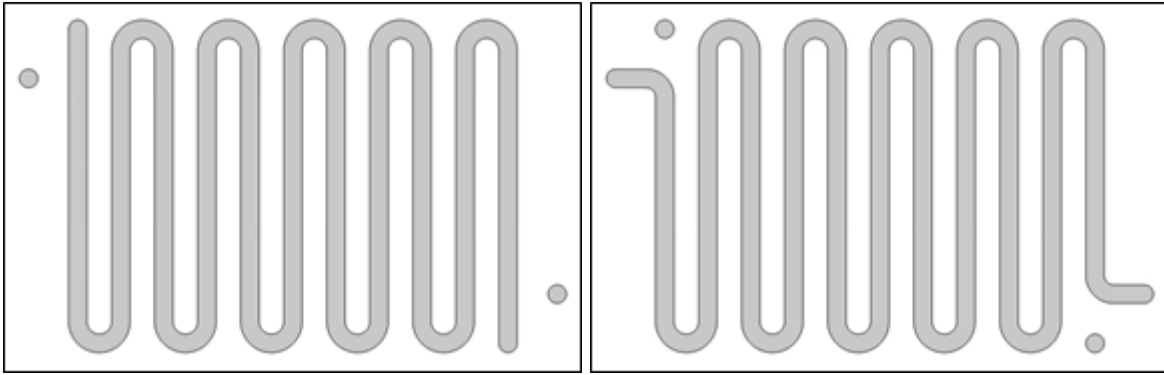


Figure 5. The wide channel serpentine channel design. The left is used for the BMF and the right for the dialysate.

2.2.1 Fabrication Methods

The fabrication was adapted from the previous work with some changes based on availability of materials and equipment. The initial designs were composed of two layers of PDMS with trenches that acted as the microfluidic channels. The PDMS layers (Sylgard® 184 Silicone Elastomer Kit) were casted in a mould made of acrylonitrile butadiene styrene (ABS) created via three-dimensional (3D)-printing on a Stratasys F370. These two sets of channels were separated by a regenerated cellulose membrane (14,000 molecular weight cut-off, Sigma). The PDMS-to-cellulose interfaces were adhered with a 1:10 uncured PDMS/toluene mixture as a glue and allowed to cure in the oven overnight.

Additional layers in stacked devices were added in the middle and assembled with PDMS layers on either end (Figure 6). The middle layers were made from PMMA sheets cut with a laser cutter (BOSS LS-1416, 30W) to form the channels and other required aspects such as through-holes for inlets and outlets. The PMMA-to-cellulose interfaces were adhered with a double-sided acrylic adhesive (3M OCA 8213) which was applied to the surface prior to laser cutting. The casing that enclosed the entire hemodialysis unit was made of laser cut PMMA and fastened with nuts and bolts. Tygon tubing (Tygon S3™ E-3603) was attached to the casing with an epoxy adhesive.

The latest design of the hemodialyzer forgoes the PDMS layers and instead uses a full piece of PMMA with holes only for inlets and outlets to cap the top and bottom layers. The PMMA-to-membrane interface was changed to also use the double-sided acrylic adhesive, regardless of the membrane used in the fabrication. Overall, PMMA sheets for the channel layers are covered with a double-sided adhesive on both sides. After the application of the adhesive, the sheets are heated in an oven at 70°C overnight to strengthen the adhesive bond. Then, all the PMMA pieces are cut with a laser cutter. These pieces are assembled with a membrane, using the attached double-sided adhesive. This entire cartridge is returned to the oven at 70°C overnight again to ensure a secure adhesive bond. This cartridge is placed between two PDMS sheets into its housing to prevent any leakages. Finally, the casing is further reinforced with an aluminum plate on either side so that the pressure is distributed evenly across the entire hemodialysis unit, to prevent the deformation that was occurring when fastening the casing with nuts and bolts.

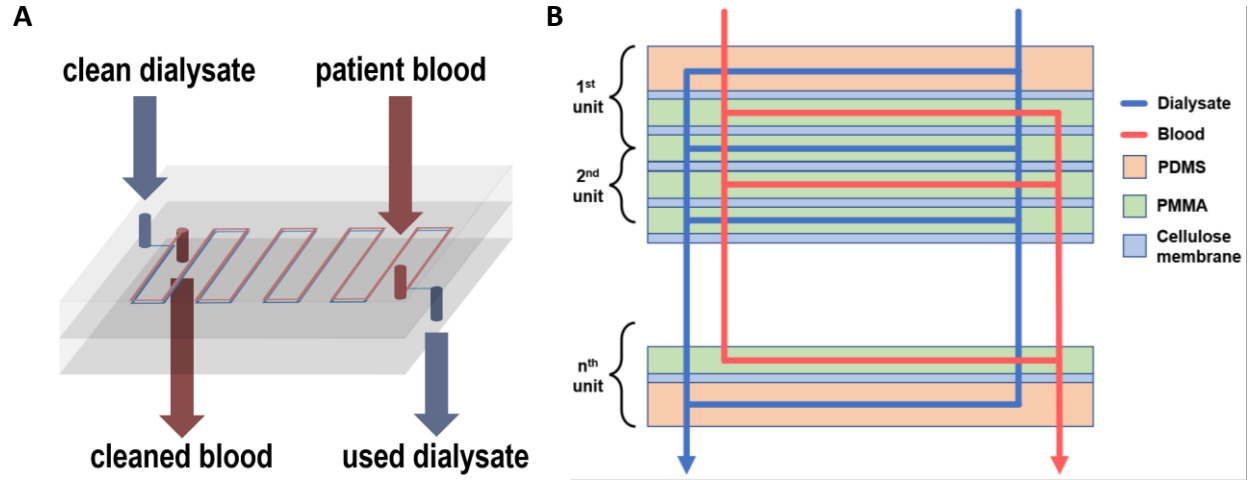


Figure 6. Schematics of dialysate and blood flow. The left (A) shows a hemodialyzer unit with one blood channel and one dialysate channel using the square microfluidic channel design. The right (B) shows the modular design of these hemodialyzers.

2.3 Hemolysis Simulations

These designs were further analyzed via computational simulations to confirm that they would not cause hemolysis in practical use. The simulations were performed using the simulation software COMSOL, with the viscosity of blood simulated based on a shear rate-dependent model so that its non-Newtonian behaviour could be captured in the simulation. For these simulations, the Quemada model at 45% hematocrit was used:

$$\mu(\dot{\gamma}) = (0.0012 \text{ Pa} \cdot \text{s}) \cdot \left(1 - \frac{1}{2} \cdot \frac{4.33 + 2.07 \sqrt{\frac{\dot{\gamma}}{1.88 \text{ s}^{-1}}}}{1 + \sqrt{\frac{\dot{\gamma}}{1.88 \text{ s}^{-1}}}} \cdot 0.45 \right)^{-2} \quad (7)$$

where μ is the viscosity and $\dot{\gamma}$ is the shear rate.⁵⁸ The Quemada model was chosen for its flexibility over a large range of shear rates. Hemolysis has been determined in literature to occur at shear stress of greater than 1,500 dynes/cm².⁴² Therefore, this value was used for the

threshold in the analysis. The entire microfluidic channel was simulated using the expected flow rates of 10 mL/min that would be used in the experiments. This resulted in a maximum wall shear stress of around 71 dyne/cm², which would not cause any hemolysis. Further simulations were performed at higher flow rates, and even at flow rates of 150 mL/min, the shear stress in the channels had still not reached the threshold for hemolysis. This assured that the microfluidic channels would not be a cause for concern with respect to hemolysis.

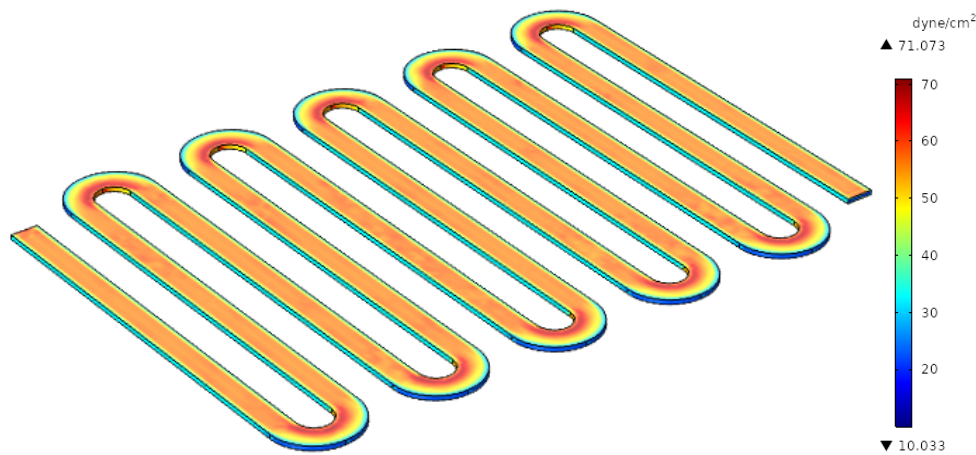


Figure 7. Shear stress simulation of the entire microfluidic channel. This simulation was performed at 10 mL/min. The numbers above and below the scale bar show the maximum and minimum wall shear stress, respectively.

However, there was another point of concern that had emerged as the fabrication process was started. The laser-cut PMMA pieces were unable to be cut with a perfectly smooth edge, which resulted in some surface roughness of the laser-cut channel walls. By introducing a randomness function into the geometry, the surface roughness of the laser-cut channels was approximated for further simulation of the shear stress. For these simulations, only the 180-degree bend was simulated since it was the region of highest shear stress in the previous

simulations. At 10 mL/min, the maximum wall shear stress was around 170 dyne/cm², which again is still much lower than the threshold for hemolysis. Similarly, higher flow rates were simulated to determine the maximum possible flow rates. For these rougher channels, the flow rates could reach nearly 100 mL/min prior to reaching the shear stress threshold for hemolysis.

From these simulations, it was determined that for the geometry of these microfluidic channels should not cause hemolysis at the flow rates intended to be used of 10 mL/min, regardless of the surface roughness introduced by the laser cutting. Higher flow rates such as 80 mL/min would also be possible without reaching this threshold.

Chapter 3 — Prototype Hemodialyzer and Performance Evaluation

3.1 Introduction

In addition to the determination of the microfluidic channels and fabrication of the hemodialyzer, a complete hemodialysis system needs to be assembled and tested so that the performance of each dialyzer can be evaluated and compared. To evaluate the performance of the dialyzer and the membrane, a blood-mimicking solution containing urea or other biologically significant molecules such as bovine serum albumin (BSA) can be flowed through the device while collecting the outlet solution. By measuring the concentration of these solutes, the rate at which they are removed from the blood-mimicking solution can be calculated and compared.

The performance of a hemodialyzer is typically measured in one of two ways. The first of which is its clearance. This is the volume of blood that is completely cleared of a substance per unit time and is typically expressed in millilitres per minute. For these devices, the main solute of interest is urea, so the urea clearance will be the main measurement to evaluate dialyzer performance, which is also the most commonly used measure of the hemodialyzer efficiency. This value is typically measured by passing a fresh blood solution of known urea concentration and a fresh dialysate solution through a dialyzer and measuring the decrease in concentration between the blood solution prior to and after passing through the dialyzer. Then, the clearance (K) can be calculated with the following equation:

$$K = Q_B \left(\frac{C_{Bpre} - C_{Bpost}}{C_{Bpre}} \right) + Q_{uf} \left(\frac{C_{Bpost}}{C_{Bpre}} \right) \quad (8)$$

where Q_B is the blood flow rate, and $C_{B_{pre}}$ and $C_{B_{post}}$ are the concentrations of the solute in the blood prior to and after dialysis respectively, and Q_{uf} is the ultrafiltration rate.⁵⁹ However, this clearance value actually changes depending on the flow rates of the blood and dialysate: the higher the flow rates, the better the clearance.^{60, 61} Typically, the dialysate flow rate is at least twice that of the blood flow rate. This is to maintain the maximum concentration gradient between the blood side and dialysate side to improve its dialysis performance.

The second measure of a hemodialyzer's performance is its mass transfer–area coefficient, or K_0A (typically rendered as KoA). This is a membrane-, solute-, and dialyzer-specific measure that can be considered the hemodialyzer's maximum clearance when the blood and dialysate flow rates are infinite.⁵⁹ This is the multiplicative product between the mass transfer coefficient K_0 and the membrane surface area A , however the KoA is the most common form used for comparing hemodialyzers. This value can be determined by measuring the clearance of a specific solute in the hemodialyzer at a specific flow rates of blood (Q_B) and dialysate (Q_D) and calculated using Equation 9. Additionally, by rearranging this formula, the clearance at any set of dialysate and blood flow rates can be predicted.

$$K_0A = \frac{Q_B Q_D}{Q_B - Q_D} \ln \left(\frac{Q_D(Q_B - K)}{Q_B(Q_D - K)} \right) \quad (9)$$

3.2 Materials and Methods

3.2.1 Cellulosic Membranes

While most modern hemodialyzers typically use synthetic membranes, cellulose membrane hemodialyzers exist as well.⁶² Cellulose is a naturally occurring polymer found in most

plants, and the surface of its disaccharide monomer, cellobiose, is rich with hydroxyl groups. Cellulose membranes themselves are commonly used in laboratory dialysis since they are inexpensive and easily purchasable in various molecular weight cut-offs. In a study of unmodified cellulose membranes in hemodialysis compared to other membranes, the unmodified cellulose membrane resulted in a significantly greater reduction in urea than the synthetic membranes.⁶³ For these reasons, a cellulose membrane was used in the previous work. However, the surface hydroxyl groups of unmodified cellulose membranes are considered to be the cause of significant activation of the complement system when blood comes into contact with it,⁴⁷ along with its associated leukopenia.^{64, 65} Despite these claims of lower biocompatibility, there is a lack of clinical evidence that there is any significant benefit of using synthetic membranes over cellulose in terms of mortality and other adverse symptoms related to dialysis.⁶² However, to prevent any problems that could arise in the future, it would be ideal to address this issue regardless. Fortunately, it is not difficult to use the hydroxyl groups themselves to functionalize the membrane to attenuate the issue of complement activation. Cellulose can be functionalized with bulky groups, such as diethylaminoethyl, which can provide steric shielding from the complement activation.⁶⁶ Similarly, smaller functional groups such as acetate can also be used, but most of the hydroxyl groups would need to be replaced to achieve a similar effect.⁴⁷ Finally, since the hemodialyzer is of a plate-like configuration instead of hollow fibres, cellulose membranes would be less expensive.

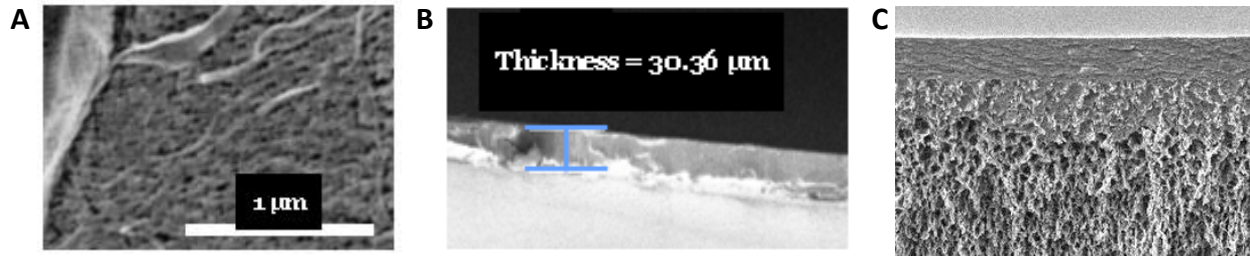


Figure 8. SEM images of the cellulose membrane. (A) The surface of the membrane. (B) The side of the membrane. (C) The expected pore structure cross section of the membrane. Adapted from MilliporeSigma.⁶⁷

3.2.2 Polycarbonate Membranes

Polycarbonate membranes are another type of membrane that have been shown to be used in hemodialysis. Studies comparing between polycarbonate membranes and regenerated cellulose membranes show that there was decreased complement activation, decreased leukopenia, and decreased release of granulocyte-derived elastase in the polycarbonate membrane when compared to the regenerated cellulose membrane.⁶⁸ These results indicate that the polycarbonate membranes are more biocompatible than unmodified cellulose membranes.

Polycarbonate membranes are also quite commonly used in the laboratory in the form of track-etched polycarbonate membranes for filtration. These track-etched membranes have consistent, cylindrical pores that are perpendicular to the membrane surface. This allows the membranes to be predictable in terms of the transport of the solutes through the membrane and increases the membrane transport as the path length is decreased. In comparison, the structure of cellulosic membranes is more sponge-like, with pores that are not easily defined. This makes predicting the dialysis through a cellulose membrane much more difficult. Furthermore,

polycarbonate membranes are commercially available much thinner than cellulose membranes, most likely due to an increased burst resistance, which can result in better hemodialytic performance.

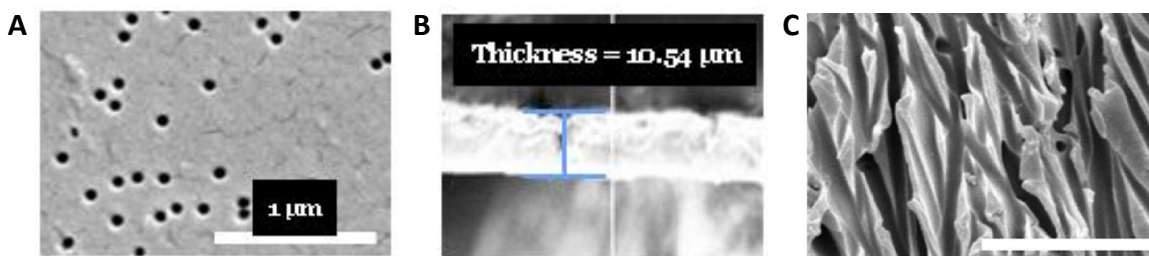


Figure 9. SEM images of the polycarbonate membrane. (A) The surface of the membrane. (B) The side of the membrane. (C) The expected pore structure cross section of the membrane. Reprinted from Ref. 69, Copyright (2017), with permission from Elsevier.⁶⁹

3.2.3 Experimental Methods

Each hemodialyzer that was fabricated was tested for its performance in hemodialysis under multiple conditions. After the hemodialysis system was assembled, attached to the peristaltic pumps, and run with water to ensure membrane hydration and the absence of any leakages, a BMF and a dialysate are flowed through the hemodialyzer countercurrently, and samples of the dialysate are taken at regular intervals. The BMF may consist of 100 mM of urea and 3.5 g/dL of BSA to represent two biologically significant molecules – one that should be removed during hemodialysis and one that should be retained during hemodialysis. The dialysate is simply the same solution as the BMF without the urea or BSA. The dialysate-side needs to mimic the blood-side in terms of electrolytes and other small molecules so that these chemicals will not diffuse into the blood which may disrupt the homeostasis of the body. Furthermore, this

ensures that there is no osmotic pressure generated from the presence of other compounds which would artificially increase the observed performance of the hemodialyzer and make it difficult to compare with existing technology.

The flow rates of the dialysate and BMF were by default both 10 mL/min. This was a restriction of the peristaltic pumps that were being used since their range of flow rates was relatively limited. The flow rate of 10 mL/min was chosen so that the flow rate could be halved or doubled and still be within the range of the capability of the pump. Furthermore, the peristaltic pump needed to be manually calibrated to the correct flow rate. This was done by measuring the volume output of the pump after one minute and adjusting as necessary. By using 10 mL/min, the output could be measured with a 10-mL graduated cylinder which was graduated to every 0.1 mL, which allows for higher accuracy of the flow rate measurement. Moreover, it has been shown that increased peristaltic pump speeds lead to higher rates of hemolysis. Therefore, the default flow rate was determined to be 10 mL/min.

The hemodialysis system was also changed to a closed-loop system for both the dialysate and blood sides so that the volumes could be minimized during testing and so that the clearance experiments could be run for much longer periods of time, such as 24 hours, without requiring large volumes of solutions to be made. With this change, it was decided that it would be more reasonable to measure the concentration of the dialysate instead of the BMF. The BMF would eventually become an increasingly complex solution, and the chances of having interfering compounds and other factors would increase by using the more complex solution between the dialysate and BMF to determine the solute concentration. Furthermore, a sample would need to

be taken from the dialysate for the determination of albumin loss regardless, so this would remove the requirement of taking samples from both sides. This change, however, required that the formula for calculating the clearance needed to be adjusted to compensate for this. First, the clearance formula would need to be adjusted to consider the volume of blood being used in the closed-loop system since it would affect the amount of urea there is to remove. Since this now reflects the concentrations in a human body during hemodialysis, a formula used to model physiological concentrations and clearance can be used:

$$\frac{d(V \times C)}{dt} = G - K \times C \quad (10)$$

where V is the total body water, C is the concentration of the solute in the blood, t is time, G is the generation rate of the solute, and K is the clearance whether by the kidneys or a hemodialyzer. The volume in the hemodialysis unit is constant with respect to time, therefore it can be factored out. Urea is not generated in the hemodialysis system, therefore the generation rate would be zero. With some rearranging of this formula, it becomes:

$$K = -\frac{V_B}{C_B} \frac{dC_B}{dt} \quad (11)$$

where the subscript B refers to the BMF. The $-dC_B/dt$ can be determined from the increase in urea concentration in the dialysate. By considering the differences in dilution of the solute between the BMF and the dialysate due to the volume differences, the increase in concentration of the dialysate can be used instead of the decrease in concentration of the BMF. Due to the diminishing concentration gradient between the dialysate and the BMF as they approach equilibrium, this rate of change will decrease as well. Therefore, the concentration of the

dialysate over time can be modelled with an increasing exponential decay function with an asymptote at the average concentration. The derivative of this function can then be used to determine the rate of change. By using the rate of change at the beginning of the dialysis, the initial concentration of the BMF can be used for C_B . This yields the final equation:

$$K = \frac{V_D}{C_{B_0}} \frac{dC_D}{dt} \Big|_{t=0} \quad (12)$$

where the subscript D refers to the dialysate, C_{B_0} is the initial BMF concentration, and $dC_D/dt|_{t=0}$ refers to the initial rate of change of C_D . The urea concentration in the dialysate is also very linear at the beginning of the hemodialysis experiment, and the slope of a linear regression can instead be used to estimate dC_D/dt , yielding a slightly lower clearance than if calculated with the actual initial rate of change.

3.2.4 Assays

The concentration of urea was determined with an assay that first uses the enzyme urease to decompose the urea into ammonia and carbonic acid.⁷⁰ The ammonia then reacts with sodium hydroxide, sodium hypochlorite, phenol, and sodium nitroprusside to form a deep blue coloured compound.⁷⁰ The resultant solution is read with an ultraviolet–visible (UV–vis) spectrophotometer (SpectraMax® M2e) and the concentration of the urea in the initial sample is determined with a standard curve.

The concentration of albumin was detected with a Bradford protein assay using the dye Coomassie blue G-250. The initial red cationic form of the dye forms a complex with protein molecules through electrostatic and hydrophobic interactions, which stabilizes in its blue anionic

form.⁷¹ This intensity of this blue colour is correlated to the amount of protein in the sample. The sample solutions incubated with this dye are read similarly with a UV–vis spectrophotometer to determine the concentration of BSA with a corresponding standard curve.

The interference of urea and albumin on each other's assay was also investigated since there would be clearance experiments using both in solution. Samples were prepared with 1 mM urea spiked with 0, 2.5, 5.0, and 10.0 g/dL of BSA and 0.1 g/dL of BSA spiked with 0, 25, 50, and 100 mM of urea and their respective assays were performed. The urea assay seemed to experience slight interference in the presence of BSA. The observed concentration of urea was raised by roughly 0.4 mM when there was 10.0 g/dL of BSA added, with a seemingly linear regression. This level of interference should not be too significant since it is relatively low compared to the typical concentrations of urea, however it should be kept in mind. The Bradford assay seemed to be unaffected by the presence of urea.

3.3 Experimental Results and Discussion

3.3.1 Urea and Albumin Clearance

The hemodialyzers fabricated with the wide serpentine channels and a regenerated cellulose membrane were tested using 100 mM of urea in phosphate-buffered saline (PBS) buffer. The flow rate of the dialysate and BMF were both set to 10 mL/min. The average clearance over four separate trials that was achieved was around 0.19 mL/min, which was more than double that of the branched serpentine design which only had a clearance of 0.070 mL/min. This demonstrates that this wide-channel hemodialyzer design is a significant improvement over the previous design.

An additional set of experiments were performed similarly using a BMF consisting of only BSA in PBS buffer to test for the diffusion of albumin across the cellulose membrane. The resulting dialysate was analyzed with a Bradford assay to visualize the presence of any proteins. This assay showed that there was no detectable amount of protein present in the dialysate over a three-hour period, indicating that albumin was unable to diffuse through the regenerated cellulose membrane. This outcome is ideal, as albumin is an important blood protein which should not be removed during hemodialysis, but also expected as the molecular weight cut-off for this membrane was 14 kDa, which is much smaller than BSA.

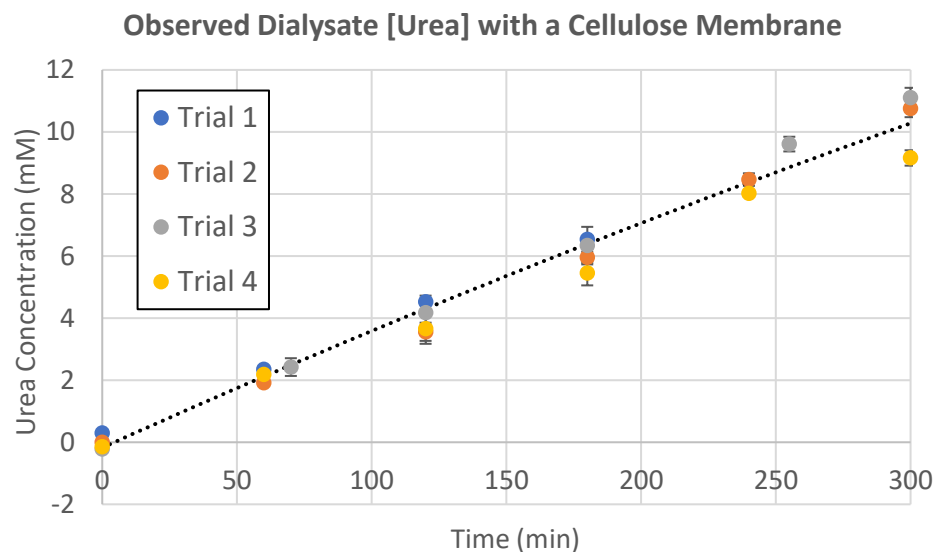


Figure 10. The dialysate urea concentration of the cellulose membrane hemodialyzer.

A longevity experiment of a hemodialyzer unit was performed by taking advantage of the university lockdown. The entire hemodialysis system was kept assembled at room temperature and filled with a 0.1% solution of sodium azide to maintain its hydration but prevent bacterial growth. After access to the laboratory was restored, which was well over six months since the

hemodialyzer was last used, another identical clearance experiment was performed on the same unit after thoroughly rinsing out the sodium azide. The urea clearance from this experiment was 0.13 mL/min, which indicated that the hemodialyzer was relatively stable for long periods of time, even while stored under a non-sterile solution. The hemodialysis system also did not suffer from any leaks or malfunctions, which was a testament to the reliability of the revised fabrication process.

However, this clearance value was still considerably low. Hence, in order to increase the clearance of the hemodialyzer, an alternate membrane with better properties was sought out to replace the regenerated cellulose membrane that was being used until now. One readily available membrane was a track-etched polycarbonate membrane with a 0.05 μm pore size. Hemodialyzers were fabricated using this membrane and tested with 100 mM urea in water. These experiments were conducted using 500 mL of dialysate and BMF and the experiments were carried out for 3 hours. The average clearance that was achieved from this set of experiments was around 0.35 mL/min, which is almost double the urea clearance that was achieved by the regenerated cellulose membrane. This showed that urea was able to be transported through the polycarbonate membrane much more easily than through the regenerated cellulose membrane.

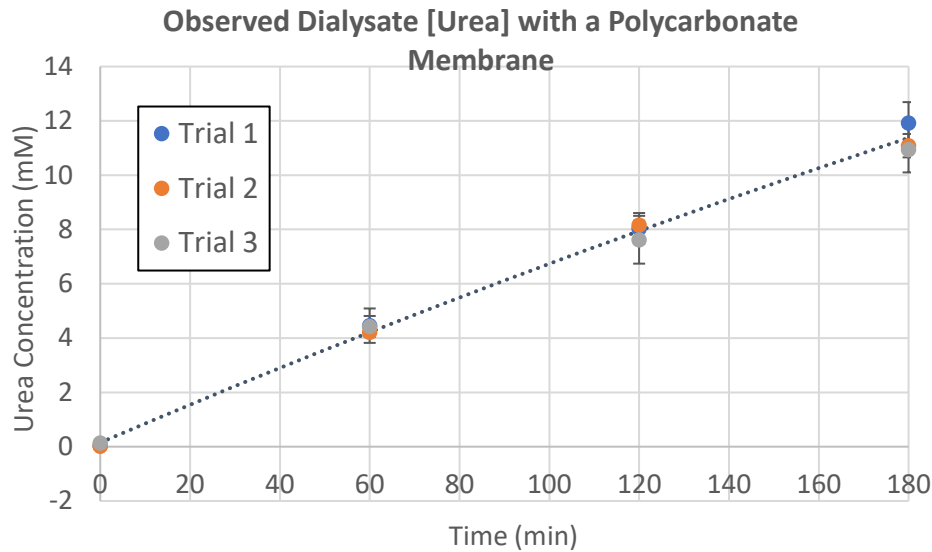


Figure 11. The urea clearance of the polycarbonate membrane hemodialyzer.

The performance of this hemodialyzer unit also needed to be tested in conditions that would be more realistic to actual hemodialysis such as in a solution with a physiological concentration of albumin which would be much more viscous than in water or buffer and possibly affect its convective transport, and eventually actual human blood to evaluate its effects on blood such as hemolysis. In preparation for the experiments that would be using whole blood, the volumes required for a clearance experiment were reduced to 100 mL of dialysate and BMF and the trial duration was reduced to 90 minutes. The volumes were reduced in anticipation of using blood to reduce the amount of blood that would need to be used, both to reduce the cost and to reduce the effects of contamination should any accidents occur. The duration was decreased as the samples would need to be taken more frequently due to the reduced volume, and there was no longer the need for a three-hour experiment. A set of experiments were conducted using this reduced volume and reduced duration with 100 mM urea in PBS buffer to confirm that the

reduction in volume did not impact the clearance values that would be calculated from the experiment. These experiments yielded an average urea clearance of 0.38 mL/min which is not statistically different from the previous data ($p = 0.3931$), demonstrating that the adjusted experiment would be consistent with the experiments using the previous conditions. This also incidentally confirms that the formula used for calculating the urea clearance is correct and scales properly as the variables are adjusted.

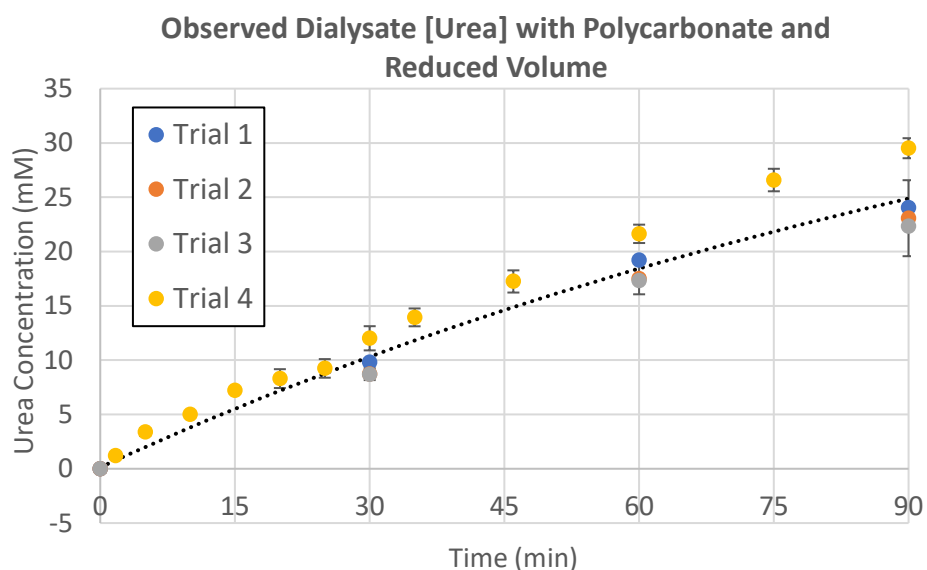


Figure 12. The urea clearance of the polycarbonate membrane hemodialyzer with reduced dialysate volume.

Using these new conditions, a set of experiments were conducted using a BMF that contained both 100 mM urea and 3.5 g/dL BSA to ensure that the presence of albumin and the associated change in viscosity does not significantly affect the function of the hemodialyzer, and again, to ensure that albumin does not easily diffuse across the polycarbonate membrane. The urea clearance was around 0.41 mL/min, which is also not significantly different from the

previous experiments ($p = 0.6329$). This indicated that the presence of the albumin did not significantly affect the performance of the hemodialyzer in terms of urea clearance.

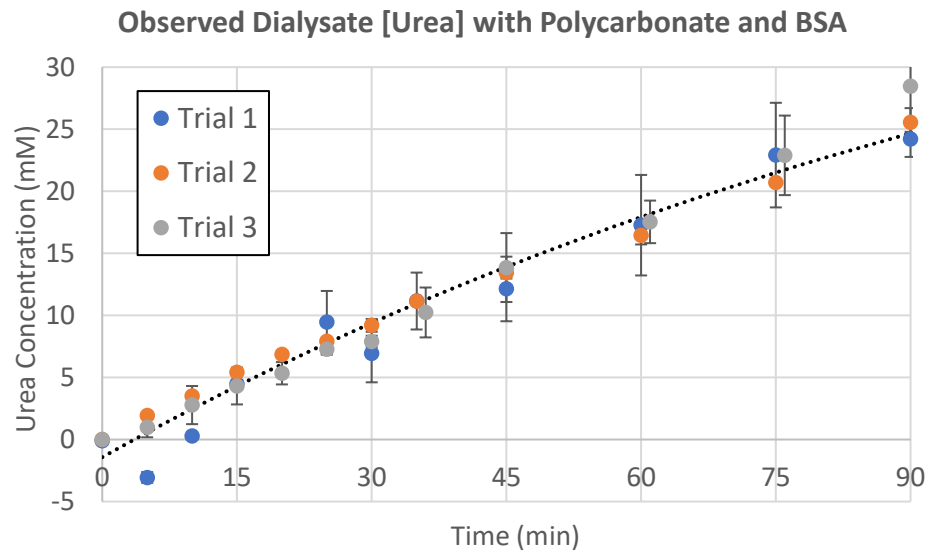


Figure 13. The urea clearance of the polycarbonate membrane hemodialyzer with BSA.

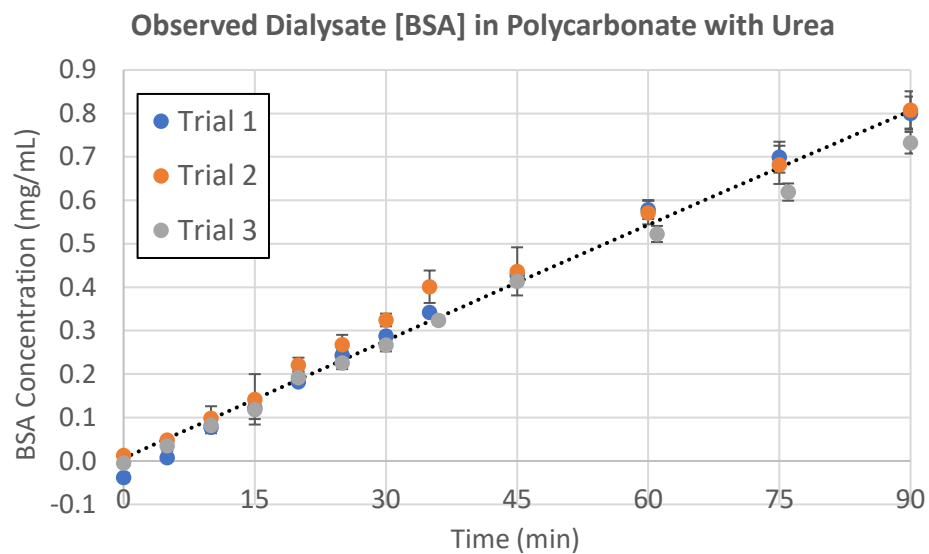


Figure 14. The BSA clearance of the polycarbonate membrane hemodialyzer.

Unlike the regenerated cellulose membrane, there was some loss of albumin into the dialysate with the polycarbonate membrane. A similar calculation was performed for the BSA, and its clearance was found to be 0.026 mL/min, which is more than 10 times lower than the clearance of urea. While ideally, there should be no loss of albumin at all, this indicates that there is at least already a natural difference in clearance between urea and albumin, which is to be expected, based on their significant difference in size. These results also imply that the polycarbonate membrane is capable of dialyzing beta-2 microglobulin, which is a 11.8-kDa immune system protein that is associated with a syndrome called “hemodialysis-related amyloidosis.”^{72, 73} This syndrome is so named since many forms of conventional hemodialysis were unable to remove molecules of this size, leading to aggregation of this protein which forms amyloid plaques in skeletal joints. Considering that the 66-kDa BSA is partially dialyzable with this membrane, it is quite likely that the much smaller beta-2 microglobulin can also be cleared with this membrane.

The polycarbonate membrane device was also tested with human whole blood to estimate its actual performance when being used with a human patient. The blood reservoir was placed in a 37°C water bath to simulate the body temperature of the patient, while the rest of the hemodialysis system remained at room temperature. The human whole blood was spiked with an extremely concentrated solution of urea so that the final concentration of the urea would be 100 mM assuming there was no urea present already present in the blood. Since the Bradford assay that was being used to detect albumin cannot differentiate between proteins, the analysis would have to group together all the blood plasma proteins. To take advantage of this

experiment which simulates a real hemodialysis session, the experiment was extended to a duration of four days. An additional sample was taken just before 24 hours, and the dialysate was replaced with a fresh solution. The blood was unchanged over the four days and the concentration of the blood was calculated from the concentration of urea in the dialysate at 24 hours. Some hemolysis was expected as extended storage of blood results in depleted energy sources such as 2,3-diphosphoglycerate which leads to the loss of cell membrane integrity and hemolysis.^{74, 75} Additionally, peristaltic pumps can cause small amounts of hemodialysis.⁷⁶ Since previous tests using whole blood on a smaller scale did not lead to any noticeable hemolysis, and there have been studies of storing anticoagulant-added whole blood for 72 hours at 25°C with minimal (0.13%) hemolysis, the experiment was started with a control blood which would be subject to the same temperatures but not dialyzed.

Unfortunately, the amount of hemolysis that occurred during the trial was much more than anticipated. There seemed to already be urea or other interferents present in the blood as the observed concentration of urea in the dialysate after the first 24 hours was around 63 mM, which should not be possible as the highest expected concentration would be 50% of the concentration of urea in the blood, or around 50 mM urea. This seemed to imply that there was around 126 mM of urea or “urea equivalents” in the blood. Additionally, with the relatively large pore size of the polycarbonate membrane, the hemoglobin subunits or perhaps hemoglobin molecules themselves from the hemolysis of the blood had also diffused across the membrane. The Bradford assay detected all the extra hemoglobin that had migrated into the dialysate and was therefore unable to even determine the concentration of blood plasma proteins. The

dialysate of the second day equilibrated to around 14 mM of “urea equivalents,” which is much lower than what should have been remaining in the blood. On the third day, the observed urea concentration in the dialysate seemed to have reached equilibrium after the first 90 minutes of dialysis. And finally, on the last day, there was no observed urea over all 90 minutes of dialysis. These results are challenging to interpret, but some conclusions can be made. The observed urea concentrations of the first 90 minutes of the experiment when the hemolysis was still minimal looked to be relatively similar to the concentrations in previous experiments, suggesting that the urea clearance may have been similar. The dialysate had observationally taken on a deep red colour after each day, including the 90 minutes of the last day, implying that hemoglobin or its subunits were able to pass through the membrane and that there was no complete clogging of the pores despite the last day having no observed urea clearance. Due to the difference in observed urea concentration at the end of the first and second days, it seems that the urea is being removed from the system in some other way. Since there have not been previous experiments that have been run for over 48 hours, it may be possible that some part of the hemodialysis system itself is able to adsorb urea when exposed to long periods of time. Another possibility is that some component of the blood, such as the cellular debris, is able to sequester the urea over time. Regardless of the reason for these unusual results, the numerical data from this experiment cannot be used for analysis of performance.

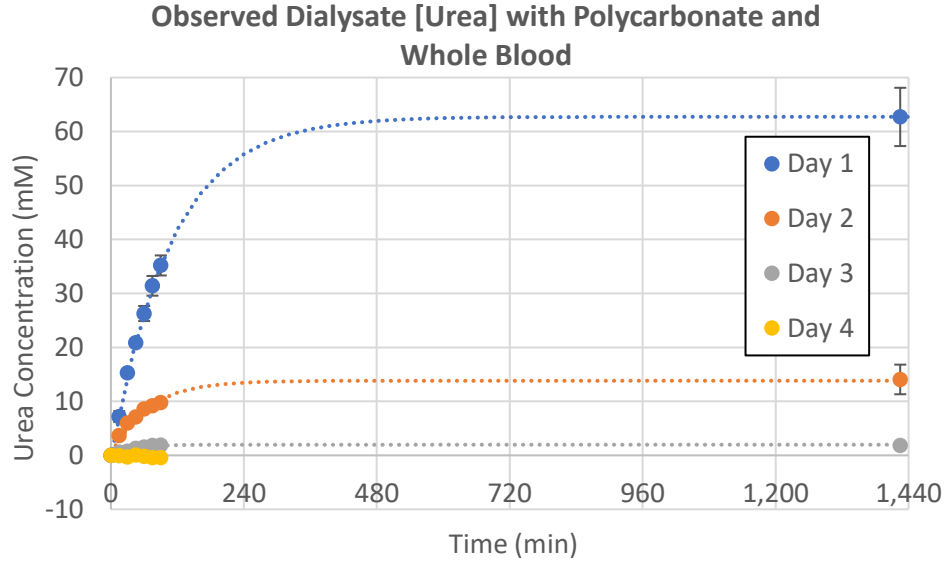


Figure 15. The urea clearance of the polycarbonate membrane hemodialyzer in whole blood.

3.3.2 Discussion of Hemodialyzer Performance

Using the data from the experiments with a BMF containing both urea and BSA, as the numerical data from the blood experiment is nonsensical, the urea clearance of the device is around 0.41 mL/min. Since the flow rates of the BMF and dialysate are much lower than normal, it would be ideal to calculate this as a KoA to compare with other hemodialyzers. The original equation for KoA has a condition where the flow rate of the dialysate cannot be the same as the flow rate of the blood due to the difference between the two being in the denominator. Since the two flow rates used in these experiments are the same, the equation must be rearranged so that it can be used. This yields the following formula for determining the KoA at equal Q_B and Q_D :

$$K_0A = -\frac{K \times Q_B}{K - Q_B}, \text{ where } Q_B = Q_D \quad (13)$$

Using this new formula, the KoA of this hemodialyzer can be calculated to be approximately 0.43 mL/min. While this does make it more easily comparable, there is still a very significant difference in membrane surface area between this microfluidic hemodialyzer (17.55 cm²) and commercial hemodialyzers which are typically around 1 m² (10,000 cm²) large. Therefore, the area must be divided from the KoA to leave only the membrane mass transfer coefficient for urea of 4.1 μm/s. When compared to a low-flux commercial dialyzer such as the Fresenius F4 which has a calculated mass transfer coefficient of 8.9 μm/s, the polycarbonate membrane is still around half as permeable to urea. However, despite it appearing to be insufficient for adequate urea clearance, this microfluidic hemodialyzer is intended to be used in a continuous hemodialysis system that would be worn everyday instead of used for 12 hours per week. That means that the microfluidic hemodialysis system would on average be in use for 14 times longer than the conventional hemodialysis system. Therefore, the polycarbonate membrane should still be viable for continuous hemodialysis even after functionalization and further manipulation of the membrane to enhance its other properties.

Another comparison that can be made is to the glomerular filtration rate of the kidney. Again, this is the rate at which fluid passes from the glomerulus into the Bowman's capsule. For solutes which freely diffuse through like urea, this is equivalent to the rate at which a solution at the same concentration as the blood passes from the glomerulus side into the Bowman's capsule side. In comparison, the urea clearance value is the rate at which blood is completely cleared of its urea, which is also equivalent to the rate at which a solution at the same concentration as the blood passes from the blood side into the dialysate side. Therefore, these two values can be

compared. Again, the surface area of the exchange area will need to be considered in both cases. The clearance per surface area of the hemodialyzer presented here is 234 mL/min/m². For the kidney, the healthy range of GFR is 90–120 mL/min/1.73 m². Since this is given over the average body surface area, it will instead need to be divided by the filtration area of the glomerulus, which is around 516.2 cm².⁷⁷ This yields a clearance per unit area of around 1744–2325 mL/min/m². This value does not consider the reabsorption of urea that occurs downstream of the Bowman's capsule before it is excreted. The tubular fluid exiting the inner medullary collecting duct contains only approximately 50% of the filtered urea,⁷⁸ therefore the effective clearance is only around half of the values above. Regardless, the current membrane is not yet as efficient as the kidney in removing urea, and more progress will need to be made to achieve that.

Finally, the current experimental system uses a closed-loop configuration for the dialysate to conserve the dialysate used for testing. However, this change does not have to be constricted to the experimental set-up. The urea clearance of the hemodialyzer does not deviate significantly from the linear regression within the dialysate urea concentration range from zero to half of the BMF urea concentration. For comparison, the average hemodialysis patient undergoes around 12–15 hours of hemodialysis weekly,⁷⁹ and typically employs a dialysate flow rate of 500 mL/min which means at least 360 litres of dialysate are required per week for hemodialysis.⁸⁰ Clinical guidelines state that the serum urea concentration should be reduced by at least 65% per hemodialysis treatment session,⁸¹ and most hemodialysis patients have a serum urea concentration of 201–300 mg/dL (33.5–50.0 mM) prior to treatment.⁸² Using the average volume of distribution as a percentage of body weight 42.1%,⁸³ and the average weight of 58,106

hemodialysis patients,⁸⁴ the urea distribution volume is around 34 L. Therefore, the highest concentration of used dialysate would only be around 28 mg/dL (4.7 mM). This is an excessive use of water and would also not be feasible for a wearable hemodialysis system. Recycling the dialysate until a substantial concentration has been achieved prior to disposal would immensely reduce the dialysate required for hemodialysis and turns out to have been suggested for situations where water needs to be conserved.⁸⁵

Chapter 4: Membrane Surface Functionalization

4.1 Introduction

Biological fouling, or biofouling, is the adsorption of biomolecules or microorganisms onto any surface exposed to biological fluids or tissue.⁸⁶ This problem can occur in most biomedical devices and systems, including hemodialysis. Adsorption of biomolecules such as proteins can cause immunological responses and even cause promote the adhesion of microorganisms which could lead to infection.⁸⁶ Furthermore, in membrane systems, biofouling on the membrane can result in blockages of the membrane pores, which would affect the permeability of the membrane and therefore its efficiency.⁸⁷ One extremely widely used method of preventing biofouling is the functionalization of the surface with polymers. The most common of these polymers is poly(ethylene glycol) (PEG).⁸⁶ PEG, which has been dubbed the “gold standard” polymer for antibiofouling, is favoured for this purpose in part owing to its low intrinsic toxicity and hydrophilicity.⁸⁸ The electrical neutrality of the added PEG is able to reduce protein fouling by reducing the electrostatic interactions that would be able to occur between the membrane surface and the charged protein domains.⁸⁶ The hydrophilicity of PEG can also reduce the nonpolar interactions between hydrophobic surfaces and nonpolar protein domains. Additionally, with PEG molecules of sufficient length, it can also provide further prevention of protein adsorption through steric hindrance.

The PEG can be grafted onto the membrane in many ways, including adding a linker onto which the PEG can be crosslinked. One possible method is to use linker chemistry to couple the

PEG to the surface of the membrane. For example, a carboxy-functionalized PEG, such as O-(2-carboxyethyl)polyethylene glycol, can be coupled to an amine group on the surface of a membrane by using 1-ethyl-3-(3-dimethylaminopropyl)carbodiimide (EDC) and N-hydroxy-succinimide (NHS). The addition of PEG on a cellulose membrane can increase its biocompatibility by displacing the hydroxyl groups and shielding the remaining groups from activating the complement system, in addition to being an antibiofouling surface.⁴⁷

The cellulose membrane was functionalized in previous work.⁵³ First, the amine linker 3-aminopropyltriethoxysilane (APTES) was added onto the cellulose membrane surface via adsorption and condensation.⁸⁹ Once the surface of the cellulose membrane had been functionalized with amine groups, these groups can be coupled with carboxy-PEG using EDC–NHS chemistry.

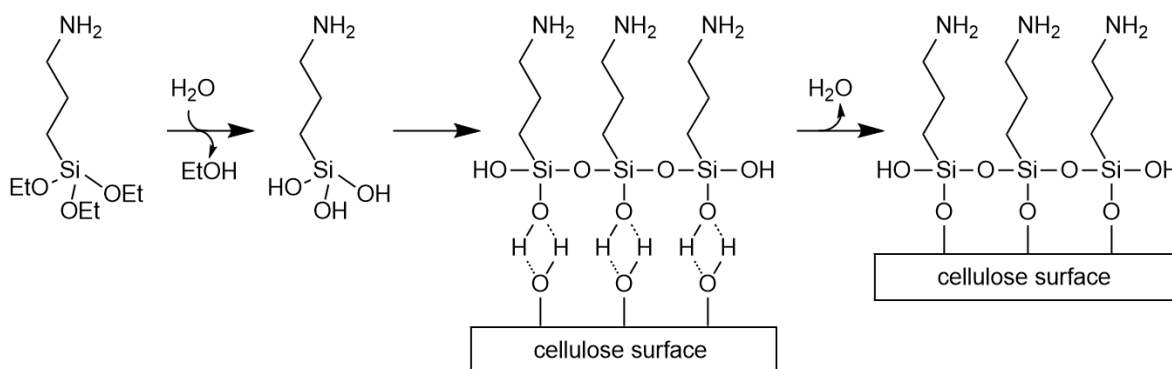


Figure 16. General scheme of the reaction between APTES and cellulose. Adapted from Magalhães et al.⁹⁰

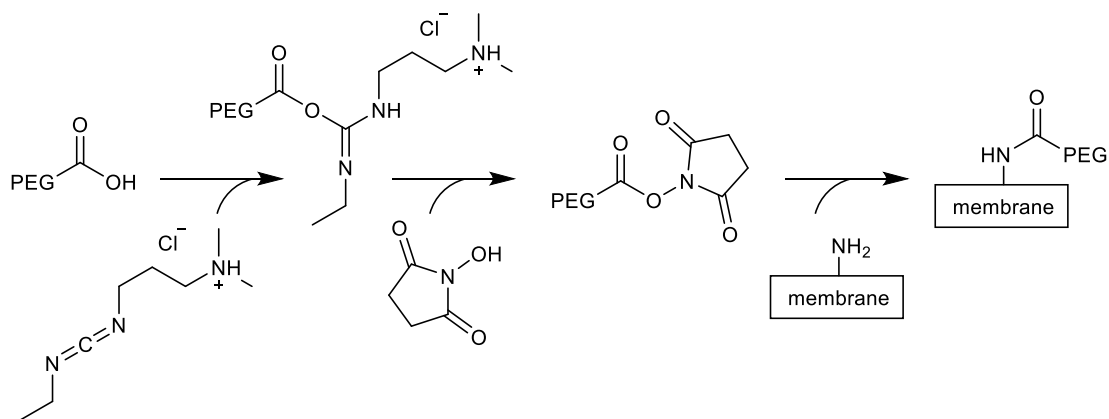


Figure 17. Scheme of membrane functionalization using EDC–NHS carbodiimide chemistry.

Adapted from Bart et al.⁹¹

4.2 Materials and Methods

The polycarbonate membrane surface was functionalized similarly to the previous work by first aminating the surface. The membrane was reacted with hexamethylenediamine (HMDA),⁹² which operates by cleaving the polymer at the carbonate ester and slowly consumes the surface of the membrane.⁹³ Therefore, this step needed to be carefully controlled so that the membrane is not completely consumed. After the surface has been decorated with amine groups, it was coupled with O-(2-carboxyethyl)polyethylene glycol, a carboxylated PEG, with the same EDC–NHS chemistry as was performed in the previous work.

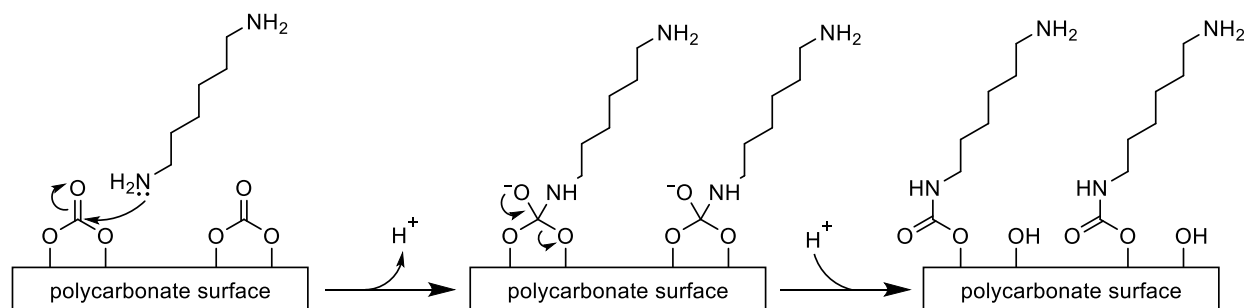


Figure 18. Scheme of the amination of polycarbonate. The left is the polycarbonate surface with the carbonate groups emphasized. The final polycarbonate is functionalized with amine groups on the surface.⁹³

4.3 Experimental Results and Discussion

The functionalization of the polycarbonate membrane was performed in a small-scale experiment to assess its viability. During the amination step, at HMDA concentrations that were too high or reaction times that were too long, the resulting membrane would disintegrate or have a very low burst strength. Therefore, the concentration and reaction time needed to be experimented with to result in a membrane that is still viable after functionalization. The contact angle of the polycarbonate membrane surface was measured to visualize its progress. Prior to any functionalization, the contact angle of the membrane was around 101°. After the amination reaction, the contact angle had reduced to around only 54°. Finally, after the addition of PEG, it reduced to 20°, indicating that the functionalization was successful. The antibiofouling properties of this PEG-functionalized membrane have yet to be tested, therefore, it must be extrapolated from the previous work.

The PEG-functionalized cellulose membrane from the previous work was demonstrated to be able to significantly lower the incidence of biofouling. Fluorescently-labelled platelets were incubated with cellulose membranes with and without PEG functionalization. The platelet counts on the functionalized membrane were 86% lower than the unmodified membrane.⁵³ This demonstrates that the addition of the PEG layer was able to significantly reduce biofouling on the surface. By considering this antibiofouling performance of PEG on the cellulose membrane

and the fact that PEG is hailed as the gold standard for antibiofouling, there is little concern that it would differ on the polycarbonate surface.

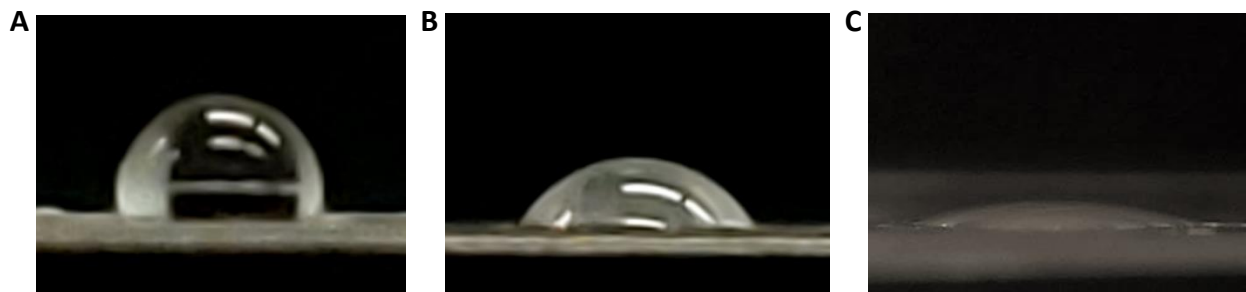


Figure 19. Contact angles of the polycarbonate membrane. (A) The untreated polycarbonate membrane. (B) The polycarbonate membrane aminated with HMDA. (C) The polycarbonate membrane functionalized with PEG.

While PEG is quite popular for its antibiofouling properties, other polymers have been proposed for similar purposes. One possible family of polymers are the zwitterionic polymers.⁹⁴ These polymers have been proposed as an alternative to PEG since it contains charged groups which can result in a stronger hydration layer and therefore more easily prevent biofouling. Therefore, in addition to experimentation with PEG, these zwitterionic polymers can also be considered for the antibiofouling functionalization.

Chapter 5: Summary and Future Work

5.1 Summary

Due to the benefits of continuous wearable hemodialysis compared to conventional hemodialysis, a small microfluidic hemodialyzer was designed for these needs. By testing the clearance of various geometries, a simple serpentine-channeled geometry was chosen for its efficient use of the surface area. The dimensions of these serpentine channels were determined by balancing the optimization for performance with the efficiency of fabrication and prevention of hemolysis.

Using both cellulose and polycarbonate membranes, the clearance of each were determined under various conditions. It was concluded that the polycarbonate membranes performed better and therefore polycarbonate was chosen for the membrane. The membrane in this microfluidic hemodialyzer was shown to be comparable to some commercial hollow-fibre hemodialyzers when it is used in a continuous setting. While the overall hemodialyzer urea clearance does not reach that of a commercial hemodialyzer, the mass transfer coefficient of the membrane shows that it has the potential to provide adequate dialysis when the flow rates are increased to that of a commercial system, ultrafiltration is applied, and the modular design is made use of to provide an increased surface area. This microfluidic hemodialyzer also uses less expensive materials and fabrication processes and can be easily modified in terms of functionalization to provide any additional surface properties that would make it more desirable.

5.2 Future Work

In addition to these findings, there are many other improvements for the polycarbonate membrane and the overall wearable hemodialysis system for which investigation has been started.

5.2.1 Pore Size Manipulation

The pore size of the current polycarbonate membrane is a bit too large as it is still able to allow the passage of important proteins such as albumin. One option to improve this is to reduce the size of these pores by depositing a thin layer of material at an angle such that it occludes part of the pore entrance. The layer needs to be uniform and anisotropic to prevent the pores from being closed. A preliminary test of depositing a 40-nm layer of chromium, followed by a 200-nm layer of gold was performed at 0°, 6°, and 12° to attempt to reduce the pore size. Unfortunately, the experiment results in completely occluded pores, possibly due to the layer being too thick and formed surface structures possibly due to the accumulation of surface charge.

Another method of having smaller pores is to track-etch a polycarbonate membrane in-house. If a custom track-etched polycarbonate membrane could be made, then the pore density and pore size could be carefully controlled, which could result in better performance.

5.2.2 Dialysate Regeneration

An important aspect of creating a portable hemodialysis system is the dialysate usage. As discussed, conventional hemodialysis uses extremely large amounts of water to achieve the performance required to treat ESRD patients. While recycling the dialysate as is can reduce the

volumes needed, the dialysate would still eventually need to be replaced. For wearable hemodialysis, a system to remove the urea along with other waste products would be required to regenerate the dialysate for reuse. One option that is already in use by the WAK is the usage of a filter which uses activated carbon and ion exchange to regenerate the dialysate. Another possible option is to use electrochemical oxidation to break down the urea into nitrogen gas and carbon dioxide, which has previously been used in wastewater treatment.⁹⁵ However, a very preliminary test was conducted and was not able to decompose urea and more research needs to be done since the presence of chloride ions may result in the generation of toxic substances.⁹⁵

5.2.3 Blood–plasma separation

One novel aspect that can be introduced into the portable hemodialysis system is the separation of the blood into plasma and a blood cell-enriched solution. As one of the restrictions of the channel parameters is the generated shear stress due to hemolysis, one possible way to mitigate this is to use another microfluidic device to first separate most of the plasma from the blood cells and to dialyze the plasma alone prior to recombining with the extracted cells. This could also increase the urea clearance since the transport of urea is dependent upon the viscosity of the solution.

Many computational simulations have been done in an attempt to design a microfluidic blood–plasma separator. Some designs were successful in separating all blood cells, however the yield of cell-free plasma was very low and probably not efficient for hemodialysis. Furthermore, these results were only tested *in silico*, and therefore may not completely reflect the problems

that could be encountered *in vitro*. Therefore, more research into better designs as well as actual *in vitro* experiments will need to be conducted.

5.2.4 Other Solutes

Currently only urea and albumin are being tested for simplicity. However, in the future, more solutes should be added into the BMF and experimented with to gain a more comprehensive view of the membrane performance. One molecule that was previously mentioned was beta-2 microglobulin, which has a molecular weight of 11.8 kDa. This molecule would probably serve as the upper bound of what should be removed from the BMF. Currently, we are using the Bradford assay to determine the albumin concentrations, but if there are other proteins introduced, this would not be a viable option. The Bradford assay has already been demonstrated to be ineffective when dealing with whole blood, so an alternative method of quantifying the amount of albumin will need to be used. Preliminary tests can be performed by only performing experiments with one protein per experiment, but it would be ideal to be able to determine the concentrations of each individual protein in complex solutions. This can be done with assay kits specific to each protein, but these are costly and may sometimes still fail in complex media such as blood.

Another molecule that can be added to the BMF is creatinine, a breakdown product produced during muscle metabolism. This molecule is already commonly used to determine renal function. Preliminary experiments of an assay to detect creatinine have already been performed (Appendix B). However, this assay would still be prone to interference from some other solutes, so clearance studies with only compatible solutes may need to be performed.

References

- [1] M. A. Perazella, "Renal Vulnerability to Drug Toxicity," *Clinical Journal of the American Society of Nephrology*, vol. 4, no. 7, p. 1275–1283, 2009.
- [2] M. J. Thomas, D. J. Fraser and T. Bowen, "Biogenesis, Stabilization, and Transport of microRNAs in Kidney Health and Disease," *Non-Coding RNA*, vol. 4, no. 4, p. 30, 2018.
- [3] A. Baig, "Biochemical Composition of Normal Urine," in *Nature Precedings*, 2011.
- [4] J. H. Salazar, "Overview of Urea and Creatinine," *Laboratory Medicine*, vol. 45, no. 1, p. e19–e20, 2014.
- [5] C. M. R. LeMoine and P. J. Walsh, "Evolution of urea transporters in vertebrates: adaptation to urea's multiple roles and metabolic sources," *Journal of Experimental Biology*, vol. 218, no. 12, p. 1936–1945, 2015.
- [6] L. A. Stevens, J. Coresh, T. Greene and A. S. Levey, "Assessing Kidney Function — Measured and Estimated Glomerular Filtration Rate," *The New England Journal of Medicine*, vol. 354, no. 23, p. 2473–2483, 2006.
- [7] C. Almeras and À. Argilés, "The General Picture of Uremia," *Seminars in Dialysis*, vol. 22, no. 4, p. 329–333, 2009.
- [8] OpenStax, "Gross Anatomy of the Kidney," in *Anatomy and Physiology*, Houston, TX, Rice University, 2013.
- [9] A. C. Webster, E. V. Nagler, R. L. Morton and P. Masson, "Chronic Kidney Disease," *The Lancet*, vol. 289, no. 10075, p. 1238–1252, 2017.
- [10] GBD 2019 Diseases and Injuries Collaborators, "Global burden of 369 diseases and injuries in 204 countries and territories, 1990–2019: a systematic analysis for the Global Burden of Disease Study 2019," *The Lancet*, vol. 396, no. 10258, p. 1204–1222, 2020.
- [11] T. Liyanage, T. Ninomiya, V. Jha, B. Neal, H. M. Patrice, I. Okpechi, M.-h. Zhao, J. Lv, A. X. Garg, J. Knight, A. Rodgers, M. Gallagher, S. Kotwal, A. Cass and V. Perkovic, "Worldwide access to treatment for end-stage kidney disease: a systematic review," *The Lancet*, vol. 385, no. 9981, p. 1975–1982, 2015.
- [12] M. A. Kabbalo, M. Canney, P. O'Kelly, Y. Williams, C. O. O'Seaghdha and P. J. Conlon, "A comparative analysis of survival of patients on dialysis and after kidney transplantation," *Clinical Kidney Journal*, vol. 11, no. 3, p. 389–393, 2018.
- [13] F. McCormick, P. J. Held and G. M. Chertow, "The Terrible Toll of the Kidney Shortage," *Journal of the American Society of Nephrology*, vol. 29, no. 12, p. 2775–2776, 2018.
- [14] S. Vadakedath and V. Kandi, "Dialysis: A Review of the Mechanisms Underlying Complications in the Management of Chronic Renal Failure," *Cureus*, vol. 9, no. 8, p. e1603, 2017.
- [15] J. Himmelfarb and T. A. Ikizler, "Hemodialysis," *The New England Journal of Medicine*, vol. 363, p. 1833–1845, 2010.
- [16] I. Baldwin, M. Baldwin, N. Fealy, M. Neri, F. Garzotto, J. C. Kim, A. Giuliani, F. Basso, F. Nalesso, A. Brendolan and C. Ronco, "Con-Current versus Counter-Current Dialysate Flow during CVVHD. A Comparative Study for Creatinine and Urea Removal," *Blood Purification*, vol. 41, p. 171–176, 2016.
- [17] C. Ronco, "Evolution of Hemodiafiltration," *Contributions to Nephrology*, vol. 158, p. 9–19, 2007.

- [18] A. Rajkomar, A. Mayer and A. Blandford, "Understanding safety–critical interactions with a home medical device through Distributed Cognition," *Journal of Biomedical Informatics*, vol. 56, p. 179–194, 2015.
- [19] United States Renal Data System, "2020 Annual Data Report: Epidemiology of Kidney Disease in the United States," USRDS, Ann Arbor, 2020.
- [20] Y.-K. Lee, K. Kim and D. J. Kim, "Current status and standards for establishment of hemodialysis units in Korea," *The Korean Journal of Internal Medicine*, vol. 28, no. 3, p. 274–284, 2013.
- [21] S. Kalim, R. Wald, A. T. Yan, M. B. Goldstein, M. Kiaii, D. Xu, A. H. Berg, C. Clish, R. Thadhani, E. P. Rhee and J. Perl, "Extended Duration Nocturnal Hemodialysis and Changes in Plasma Metabolite Profiles," *Clinical Journal of American Society of Nephrology*, vol. 13, no. 3, p. 436–444, 2018.
- [22] K. Gerasimoula, L. Lefkothea, L. Maria, A. Victoria, T. Paraskevi and P. Maria, "Quality of Life in Hemodialysis Patients," *Materia Sociomedica*, vol. 27, no. 5, p. 305–309, 2015.
- [23] H. Schiff, S. M. Lang and R. Fischer, "Daily Hemodialysis and the Outcome of Acute Renal Failure," *The New England Journal of Medicine*, vol. 346, p. 305–310, 2002.
- [24] S. Koshikawa, T. Akizawa, A. Saito and K. Kurokawa, "Clinical Effect of Short Daily In-Center Hemodialysis," *Nephron Clinical Practice*, vol. 95, no. 1, p. c23–c30, 2003.
- [25] Z. J. Twardowski, "Daily dialysis: is this a reasonable option for the new millennium?," *Nephrology Dialysis Transplantation*, vol. 16, no. 7, p. 1321–1324, 2001.
- [26] F. O. Finkelstein, B. Schiller, R. Daoui, T. W. Gehr, M. A. Kraus, J. Lea, Y. Lee, B. W. Miller, M. Sinsakul and B. L. Jaber, "At-home short daily hemodialysis improves the long-term health-related quality of life," *Kidney International*, vol. 82, no. 5, p. 561–569, 2012.
- [27] D. Zepeda-Orozco and R. Quigley, "Dialysis disequilibrium syndrome," *Pediatric Nephrology*, vol. 27, no. 12, p. 2205–2211, 2012.
- [28] L.-A. Topfer, "Wearable Artificial Kidneys for End-Stage Kidney Disease," in *CADTH Issues in Emerging Health Technologies*, Ottawa, Canadian Agency for Drugs and Technologies in Health, 2016.
- [29] V. Gura, M. B. Rivara, S. Bieber, R. Munshi, N. C. Smith, L. Linke, J. Kundzins, M. Beizai, C. Ezon, L. Kessler and J. Himmelfarb, "A wearable artificial kidney for patients with end-stage renal disease," *JCI Insight*, vol. 1, no. 8, p. e86397, 2016.
- [30] M. Wester, K. G. Gerritsen, F. Simonis, W. H. Boer, D. H. Hazenbrink, K. R. Vaessen, M. C. Verhaar and J. A. Joles, "A regenerable potassium and phosphate sorbent system to enhance dialysis efficacy and device portability: a study in awake goats," *Artificial Organs*, vol. 38, no. 12, p. 998–1006, 2014.
- [31] R. Giordano and R. Corder, "Portable hemodialysis machine and disposable cartridge". United States of America Patent 10,155,078.
- [32] C. W. McIntyre and J. O. Burton, "Dialysis," *The BMJ*, vol. 348, p. bmj.g2, 2014.
- [33] H. Espinoza-Gómez and S. W. Lin, "Development of Hydrophilic Ultrafiltration Membrane from Polysulfone-Polyvinylpyrrolidone," *Revista de la Sociedad Química de México*, vol. 47, no. 1, p. 53–57, 2003.
- [34] B. Su, S. Sun and C. Zhao, "Polyethersulfone Hollow Fiber Membranes for Hemodialysis," in *Progress in Hemodialysis: From Emergent Biotechnology to Clinical Practice*, A. Carpi, C. Donadio and G. Tramonti, Eds., 2011.

- [35] Y. Higaki, M. Kobayashi, D. Murakami and A. Takahara, "Anti-fouling behavior of polymer brush immobilized surfaces," *Polymer Journal*, vol. 48, no. 4, p. 325–331, 2016.
- [36] L. W. McKeen, "Markets and Applications for Films, Containers, and Membranes," in *Permeability Properties of Plastics and Elastomers*, 3rd ed., Chadds Ford, PA: William Andrew, 2012, p. 59–75.
- [37] K. Sakai, "Dialysis membranes for blood purification," *Frontiers of Medical and Biological Engineering*, vol. 10, no. 2, p. 117–129, 2000.
- [38] Z. J. Twardowski, "Dialyzer Reuse—Part II: Advantages and Disadvantages," *Seminars in Dialysis*, vol. 19, no. 3, p. 217–226, 2006.
- [39] D. H. Krieter and B. Canaud, "High permeability of dialysis membranes: what is the limit of albumin loss?," *Nephrology Dialysis Transplantation*, vol. 18, no. 4, p. 651–654, 2003.
- [40] B. J. Manns, K. Taub, R. M. A. Richardson and C. Donaldson, "To Reuse or not to Reuse?: An Economic Evaluation of Hemodialyzer Reuse Versus Conventional Single-use Hemodialysis for Chronic Hemodialysis Patients," *International Journal of Technology Assessment in Health Care*, vol. 18, no. 1, p. 81–93, 2002.
- [41] G. R. Bolton, A. W. Boesch and M. J. Lazzara, "The effects of flow rate on membrane capacity: Development and application of adsorptive membrane fouling models," *Journal of Membrane Science*, vol. 279, no. 1–2, p. 625–634, 2006.
- [42] L. B. Leverett, J. D. Hellums, C. P. Alfrey and E. C. Lynch, "Red Blood Cell Damage by Shear Stress," *Biophysical Journal*, vol. 12, no. 3, p. 257–273, 1972.
- [43] S. Haroon and A. Davenport, "Choosing a dialyzer: What clinicians need to know," *Hemodialysis International*, vol. 22, no. S2, p. S65–S74, 2018.
- [44] G. D. Ross, Ed., *Immunobiology of the Complement System: An Introduction for Research and Clinical Medicine*, Orlando, FL: Academic Press, 2014.
- [45] Z. Dembic, *The Cytokines of the Immune System: The Role of Cytokines in Disease Related to Immune Response*, San Diego, CA: Elsevier Science, 2015.
- [46] C. Ronco and R. Bellomo, "Principles of solute clearance during continuous renal replacement therapy," in *Critical Care Nephrology*, C. Ronco and R. Bellomo, Eds., New York, Kluwer Academic Publishers, 1998, p. 1213–1223.
- [47] W. R. Clark, R. J. Hamburger and M. J. Lysaght, "Effect of membrane composition and structure on solute removal and biocompatibility in hemodialysis," *Kidney International*, vol. 56, no. 6, p. 2005–2015, 1999.
- [48] R. Sam, "Hemodialysis: Diffusion and Ultrafiltration," *Austin Journal of Nephrology and Hypertension*, vol. 1, no. 2, p. 1010, 2014.
- [49] A. Piry, A. Heino, W. Kühnl, T. Grein, S. Ripperger and U. Kulozik, "Effect of membrane length, membrane resistance, and filtration conditions on the fractionation of milk proteins by microfiltration," *Journal of Dairy Science*, vol. 95, no. 4, p. 1590–1602, 2012.
- [50] N. J. Ofsthun and J. K. Leypoldt, "Ultrafiltration and Backfiltration during Hemodialysis," *Artificial Organs*, vol. 19, no. 11, p. 1143–1161, 1995.
- [51] H. Schiffli, "High-Flux Dialyzers, Backfiltration, and Dialysis Fluid Quality," *Seminars in Dialysis*, vol. 24, no. 1, p. 1–4, 2011.

- [52] W. Li, W. Xing and N. Xu, "Modeling of relationship between water permeability and microstructure parameters of ceramic membranes," *Desalination*, vol. 192, no. 1–3, p. 340–345, 2006.
- [53] I. R. Ausri, E. M. Feygin, C. Q. Cheng, Y. Wang, Z. Y. Lin and X. S. Tang, "A highly efficient and antifouling microfluidic platform for portable hemodialysis devices," *MRS Communications*, vol. 8, p. 474–479, 2018.
- [54] C. Ronco, A. Brendolan, C. Crepaldi, M. Rodighiero and M. Scabardi, "Blood and Dialysate Flow Distributions in Hollow-Fiber Hemodialyzers Analyzed by Computerized Helical Scanning Technique," *Journal of the American Society of Nephrology*, vol. 13, no. suppl 1, p. S53–S61, 2002.
- [55] C. J. Pipe, T. S. Majmudar and G. H. McKinley, "High shear rate viscometry," *Rheologica Acta*, vol. 47, no. 5–6, p. 621–642, 2008.
- [56] C. S. Thompson and A. R. Abate, "Adhesive-based bonding technique for PDMS microfluidic devices," *Lab on a Chip*, vol. 13, no. 4, p. 632–635, 2013.
- [57] P. Connes, T. Alexy, J. Detterich, M. Romana, M. D. Hardy-Dessources and S. K. Ballas, "The role of blood rheology in sickle cell disease," *Blood Reviews*, vol. 30, no. 2, p. 111–118, 2016.
- [58] A. Skiadopoulos, P. Neofytou and C. Housiadas, "Comparison of blood rheological models in patient specific cardiovascular system simulations," *Journal of Hydrodynamics, Ser. B*, vol. 29, no. 2, p. 293–304, 2017.
- [59] C. C. Magee, J. K. Tucker and A. K. Singh, Eds., *Core Concepts in Dialysis and Continuous Therapies*, Boston, MA: Springer, 2016.
- [60] S. M. Cha and H. S. Min, "The Effect of Dialysate Flow Rate on Dialysis Adequacy and Fatigue in Hemodialysis Patients," *Journal of Korean Academy of Nursing*, vol. 46, no. 5, p. 642–652, 2016.
- [61] S. R. Borzou, M. Gholyaf, M. Zandiha, R. Amini, M. T. Goodarzi and B. Torkaman, "The effect of increasing blood flow rate on dialysis adequacy in hemodialysis patients," *Saudi Journal of Kidney Diseases and Transplantation*, vol. 20, no. 4, p. 639–642, 2009.
- [62] A. M. MacLeod, M. K. Campbell, J. D. Cody, C. Daly, A. Grant, I. Khan, K. S. Rabindranath, L. Vale and S. A. Wallace, "Cellulose, modified cellulose and synthetic membranes in the haemodialysis of patients with end-stage renal disease," *Cochrane Database of Systematic Reviews*, no. 3, 2005.
- [63] R. A. Ward, R. M. Schaefer, D. Falkenhagen, M. S. Joshua, A. Heidland, H. Klinkmann and H. J. Gurland, "Biocompatibility of a new high-permeability modified cellulose membrane for haemodialysis," *Nephrology Dialysis Transplantation*, vol. 8, no. 1, p. 47–53, 1993.
- [64] L. C. Smeby, T. E. Widerøe, T. Balstad and S. Jørstad, "Biocompatibility Aspects of Cellophane, Cellulose Acetate, Polyacrylonitrile, Polysulfone and Polycarbonate Hemodialyzers," *Blood Purification*, vol. 4, no. 1–3, p. 93–101, 1986.
- [65] F. Poppelaars, B. Faria, M. Gaya da Costa, C. F. M. Franssen, W. J. van Son, S. P. Berger, M. R. Daha and M. A. Seelen, "The Complement System in Dialysis: A Forgotten Story?," *Frontiers in Immunology*, vol. 9, no. 71, 2018.
- [66] L. Lucchi, D. Bonucchi, M. A. Acerbi, G. Cappelli, A. Spattini, M. Innocenti, A. Castellani and E. Lusvarghi, "Improved Biocompatibility by Modified Cellulosic Membranes: The Case of Hemophan," *Artificial Organs*, vol. 13, no. 5, p. 417–421, 2008.
- [67] MilliporeSigma, "Ultrafiltration Discs, 30 kDa NMW | PLTK04310," Merck KGaA, 2021. [Online]. Available: https://www.emdmillipore.com/CA/en/product/Ultrafiltration-Discs-30kDa-NMW,MM_NF-PLTK04310. [Accessed April 2021].

- [68] F. Knudsen, A. H. Nielsen, J. O. Pedersen, N. Grunnet and C. Jersild, "Biocompatibility of a New Polycarbonate Dialysis Membrane," *Blood Purification*, vol. 4, no. 1–3, p. 142–146, 1986.
- [69] A. T. Servi, E. Guillen-Burrieza, D. M. Warsinger, W. Livernois, K. Notarangelo, J. Kharraz, J. H. Lienhard V, H. A. Arafat and K. K. Gleason, "The effects of iCVD film thickness and conformality on the permeability and wetting of MD membranes," *Journal of Membrane Science*, vol. 523, p. 470–479, 2017.
- [70] P. L. Searle, "The Berthelot or Indophenol Reaction and Its Use in the Analytical Chemistry of Nitrogen," *The Analyst*, vol. 109, no. 5, p. 549–568, 1984.
- [71] P. N. Brady and M. A. Macnaughtan, "Evaluation of Colorimetric Assays for Analyzing Reductively Methylated Proteins: Biases and Mechanistic Insights," *Analytical Biochemistry*, vol. 491, p. 43–51, 2015.
- [72] L. Li, M. Dong and X. G. Wang, "The Implication and Significance of Beta 2 Microglobulin: A Conservative Multifunctional Regulator," *Chinese Medical Journal*, vol. 129, no. 4, p. 448–455, 2016.
- [73] Y. Hirakura and B. L. Kagan, "Pore formation by beta-2-microglobulin: A mechanism for the pathogenesis of dialysis associated amyloidosis," *Amyloid*, vol. 8, no. 2, p. 94–100, 2001.
- [74] D. B. Kim-Shapiro, J. Lee and M. T. Gladwin, "Storage Lesion. Role of Red Cell Breakdown," *Transfusion*, vol. 51, no. 4, p. 844–851, 2011.
- [75] T. Kanias and M. T. Gladwin, "Nitric oxide, hemolysis, and the red blood cell storage lesion: Interactions between transfusion, donor, and recipient," *Transfusion*, vol. 52, no. 7, p. 1388–1392, 2012.
- [76] Cole Parmer, "Shear-Sensitive Pumping with Peristaltic Pumps," Cole-Parmer Canada Company, Montreal, QC, 2019.
- [77] A. Bohle, B. Aeikens, A. Eenboom, L. Fronholt, W. R. Plate, J. C. Xiao, A. Greschniok and M. Wehrmann, "Human glomerular structure under normal conditions and in isolated glomerular disease," *Kidney International Supplements*, vol. 67, p. S186–S188, 1998.
- [78] I. D. Weiner, W. E. Mitch and J. M. Sands, "Urea and Ammonia Metabolism and the Control of Renal Nitrogen Excretion," *Clinical Journal of the American Society of Nephrology*, vol. 10, no. 8, p. 1444–1458, 2015.
- [79] M. B. Rivara, S. V. Adams, S. Kuttykrishnan, K. Kalantar-Zadeh, O. A. Arah, A. K. Cheung, R. Katz, M. Z. Molnar, V. Ravel, M. Soohoo, E. Streja, J. Himmelfarb and R. Mehrotra, "Extended-hours hemodialysis is associated with lower mortality risk in patients with end-stage renal disease," *Kidney International*, vol. 90, no. 6, p. 1312–1320, 2016.
- [80] M. Albalade, R. Pérez-García, P. de Sequera, E. Corchete, R. Alcazar, M. Ortega and M. Puerta, "Is it useful to increase dialysate flow rate to improve the delivered Kt?," *BMC Nephrology*, vol. 16, 2015.
- [81] H. Adas, R. Al-Ramahi, N. Jaradat and R. Badran, "Assessment of adequacy of hemodialysis dose at a Palestinian hospital," *Saudi Journal of Kidney Disease and Transplantation*, vol. 25, no. 2, p. 438–442, 2014.
- [82] N. ul Amin, R. T. Mahmood, M. J. Asad, M. Zafar and A. M. Raja, "Evaluating Urea and Creatinine Levels in Chronic Renal Failure Pre and Post Dialysis: A Prospective Study," *Journal of Cardiovascular Disease*, vol. 2, no. 2, 2014.

- [83] F. Maduell, F. Sigüenza, A. Caridad, F. Miralles and F. Serrato, "Analysis of Urea Distribution Volume in Hemodialysis," *Nephron*, vol. 66, p. 312–316, 1994.
- [84] T. I. Chang, V. Ngo, E. Streja, J. A. Chou, A. R. Tortorici, T. H. Kim, T. W. Kim, M. Soohoo, D. Gillen, C. M. Rhee, C. P. Kovesdy and K. Kalantar-Zadeh, "Association of body weight changes with mortality in incident hemodialysis patients," *Nephrology Dialysis Transplantation*, vol. 32, no. 9, p. 1549–1558, 2017.
- [85] J. G. Heaf, M. Axelsen and R. S. Pedersen, "Multipass haemodialysis: a novel dialysis modality," *Nephrology Dialysis Transplantation*, vol. 28, no. 5, p. 1255–1264, 2013.
- [86] S. Lowe, N. M. O'Brien-Simpson and L. A. Connal, "Antibiofouling polymer interfaces: poly(ethylene glycol) and other promising candidates," *Polymer Chemistry*, vol. 6, no. 2, p. 198–212, 2015.
- [87] K. Yamamoto, M. Hiwatari, F. Kohori, K. Sakai, M. Fukuda and T. Hiyoshi, "Membrane fouling and dialysate flow pattern in an internal filtration-enhancing dialyzer," *Journal of Artificial Organs*, vol. 8, no. 3, p. 195–205, 2005.
- [88] K. Knop, R. Hoogenboom, D. Fischer and U. S. Schubert, "Poly(ethylene glycol) in Drug Delivery: Pros and Cons as Well as Potential Alternatives," *Angewandte Chemie International Edition*, vol. 49, no. 36, p. 6288–6308, 2010.
- [89] H. Khanjanzadeh, R. Behrooz, N. Bahramifar, W. Gindl-Altmutter, M. Bacher, M. Edler and T. Griesser, "Surface Chemical Functionalization of Cellulose Nanocrystals by 3-aminopropyltriethoxysilane," *International Journal of Biological Macromolecules*, vol. 106, p. 1288–1296, 2018.
- [90] S. Magalhães, L. Alves, B. Medronho, A. C. Fonseca, A. Romano, J. F. J. Coelho and M. Norgren, "Brief Overview on Bio-Based Adhesives and Sealants," *Polymers*, vol. 11, no. 10, p. 1685, 2019.
- [91] J. Bart, R. Tiggelaar, M. Yang, S. Schlautmann, H. Zuilhof and H. Gardeniers, "Room-temperature intermediate layer bonding for microfluidic devices," *Lab on a Chip*, vol. 9, p. 3481–3488, 2009.
- [92] V. VanDelinder, D. R. Wheeler, L. J. Small, M. T. Brumbach, E. D. Spoerke, I. Henderson and G. D. Bachand, "Simple, Benign, Aqueous-Based Amination of Polycarbonate Surfaces," *ACS Applied Materials & Interfaces*, vol. 7, no. 10, p. 5643–5649, 2015.
- [93] S. Singh, Y. Lei and A. Schober, "Direct extraction of carbonyl from waste polycarbonate with amines under environmentally friendly conditions: scope of waste polycarbonate as a carbonylating agent in organic synthesis," *RSC Advances*, vol. 5, no. 5, p. 3454–3460, 2015.
- [94] M. Kobayashi, Y. Terayama, H. Yamaguchi, M. Terada, D. Murakami, K. Ishihara and A. Takahara, "Wettability and Antifouling Behavior on the Surfaces of Superhydrophilic Polymer Brushes.," *Langmuir*, vol. 28, no. 18, p. 7212–7222, 2012.
- [95] E. Urbańczyk, M. Sowa and W. Simka, "Urea removal from aqueous solutions—a review," *Journal of Applied Electrochemistry*, vol. 46, p. 1011–1029, 2016.
- [96] B. D. Toora and G. Rajagopal, "Measurement of creatinine by Jaffe's reaction — Determination of concentration of sodium hydroxide for maximum color development in standard, urine and protein free filtrate of serum," *Indian Journal of Experimental Biology*, vol. 40, p. 352–354, 2002.
- [97] H. H. Taussky and G. Kurzmann, "A microcolorimetric determination of creatine in urine by the Jaffe reaction," *Journal of Biological Chemistry*, vol. 208, no. 2, p. 853–861, 1954.

Appendices

Appendix A: Reduction of Membrane Thickness

As discussed while examining the equations for diffusive and convective transport in hemodialysis, the thickness of the membrane factors into both the diffusive and convective clearance of the resulting hemodialyzer. As the thickness of the membrane increases, so does the path length of the solutes that need to be transported across the membrane. This results in decreased flux of that solute and therefore, decreased clearance. The reduction of membrane thickness was investigated for both the cellulose and polycarbonate membranes.

The cellulose membrane that was being used for hemodialysis was around 50 μm thick when hydrated. One option to reduce the thickness was to slowly etch the surface layer away until a desirable thickness was reached. Preliminary tests were performed using plasma etching with a gas flow rate of 20 sccm, a pressure of 50 mTorr, and a radio frequency power of 100 W. This resulted in an etching rate of 1.5 $\mu\text{m}/\text{min}$ which was performed for 18 min, decreasing the thickness by from 50 μm to around 27 μm . The first test was performed on a small piece of cellulose membrane. This thickness of this piece of cellulose membrane seemed to be reduced significantly and it had also changed from clear to translucent during the etching process. This opacity change may have occurred due to the introduction of surface morphology. As more surface roughness was introduced, the surface would diffuse the incoming light more, leading to a translucent appearance. This piece of membrane also became more fragile after the processing. The fabrication would have been more difficult as the membrane would be much more

susceptible to tearing. Therefore, a second test was performed with the membrane adhered to one side of PDMS as structural support prior to the plasma etching. The similarly small piece of cellulose membrane attached to PDMS was treated with oxygen plasma to test for any changes during the treatment, such as a loss of adhesion. As this did not seem to compromise the adhesion, a full-sized PDMS-mounted cellulose membrane was prepared for treatment with oxygen plasma. However, at this full size, the cellulose membrane seemed to shrink noticeably, causing the PDMS to curve inwards. This may be caused due to using excessive power or oxygen during the plasma treatment which possibly caused the collapse of the pore structure of the cellulose, which may be corrected with an adjusted protocol. However, with the replacement of the 50- μm cellulose membrane with a 10- μm polycarbonate membrane, it seemed that it would not be possible to reduce the thickness of the cellulose membrane such that it could outperform the new polycarbonate membrane.

The polycarbonate was only 10 μm thick, however experiments that attempted to further reduce the thickness were performed. While investigating the chemical reaction used to functionalize the polycarbonate membrane with amine groups, it was noted that the reaction was destructive and results in polymer scission. This meant that this reaction would be able to etch the surface of the polycarbonate membrane. Thus, a small-scale test was performed to measure the reduction of the membrane thickness. A small piece of polycarbonate membrane was reacted in 5% and 10% solutions of HMDA for 24 hours. The membrane in the 10% solution had a complete loss of structural integrity and was not possible to handle as it fell apart with any contact, however the membrane in the 5% solution was still easily handleable. Therefore, a

scanning electron microscope (SEM) micrograph was taken of an unmodified polycarbonate membrane and the membrane reacted with 5% HMDA for 24 hours. This thinned membrane had a reduced thickness of around 4 μm and appeared to be much more handleable than the plasma-etched regenerated cellulose membrane. There also seemed to be the side effect of pore widening, with the pores increasing from around 50 nm to around 120 nm. Despite the increased size of the pores, an experiment was performed where an assembled polycarbonate hemodialysis unit was thinned and functionalized *in-situ* using the same protocol. However, after the functionalization was complete and the excess HMDA was being rinsed from the unit, the membrane ruptured catastrophically from the transmembrane pressure generated from the pumps. While reinspecting the membranes from the small-scale test, it was noticed that the long reaction times in the HMDA had resulted in a significant loss of tensile strength in the membrane. This unfortunately suggested that chemical etching to reduce the thickness of the polycarbonate membrane was not an option. Retrospectively, disregarding of the shrinkage of the plasma-etched cellulose membrane, its fragility suggests that it likely would not have been able to withstand these pressures either.

Appendix B: Creatinine Assay

The creatinine assay was adapted from published assays using the Jaffe reaction.^{96, 97} A solution of 2.5 mg/mL creatinine HCl was prepared as a standard. An additional solution of 0.75 M sodium hydroxide (NaOH) was prepared. In a 96-well plate, 150 μ L of the sample was added, followed 50 μ L of a 1:1 mixture of 1% picric acid and 0.75 M NaOH. After 20 minutes, the samples were read with a spectrophotometer at 550 nm. This resulted in a very well-defined curve with a linear region of around 0–0.5 mg/mL.